Title
ATOMIC BEAM MEASUREMENT OF THE ISOTOPE SHIFTS IN l27Cs, l29Cs, 133Cs, 134Cs, 134mCs, AND 137Cs

Author
Wang, Edmond Ghen-ching.

Publication Date
1968-09-27

UCRL-18434

cy. 2

University of California

Ernest O. Lawrence Radiation Laboratory

ATOMIC BEAM MEASUREMENT OF THE ISOTOPE SHIFTS IN ^{127}Cs, ^{129}Cs, ^{133}Cs, ^{134}Cs, ^{134m}Cs, and ^{137}Cs

Edmond Chen-ching Wang

(Ph. D. Thesis)

September 27, 1968

Berkeley, California

DISCLAIMER

UCRL-18434

UNIVERSITY OF CALIFORNIA

Lawrence Radiation Laboratory
Berkeley, California

AEC Contract No. W-7405-eng-48

ATOMIC BEAM MEASUREMENT OF THE ISOTOPE SHIFTS IN ^{127}Cs, ^{129}Cs, ^{133}Cs, ^{134}Cs, ^{134m}Cs, and ^{137}Cs

Edmond Chen-ching Wang

(Ph.D. Thesis)

September 27, 1968

ATOMIC BEAM MEASUREMENT OF THE ISOTOPE SHIFTS IN ^{127}Cs, ^{129}Cs, ^{133}Cs, ^{134}Cs, ^{134m}Cs, and ^{137}Cs

Contents

ATOMIC BEAM MEASUREMENT OF THE ISOTOPE SHIFTS IN ^{127}Cs, ^{129}Cs, ^{133}Cs, ^{134}Cs, ^{134m}Cs, and ^{137}Cs

Edmond Chen-ching Wang

Lawrence Radiation Laboratory
University of California
Berkeley, California

ABSTRACT

A new atomic-beam technique has been employed to measure the isotope shifts of five radioactive cesium isotopes relative to the stable isotope ^{133}Cs. The shifts (in 10^{-3} cm^{-1}) in the D_1 line are found to be

Isotope:	^{127}Cs	^{129}Cs	^{134}Cs	^{134m}Cs	^{137}Cs
IS :	+5.9(1.5)	+2.8(1.5)	+1.8(1.0)	-2.2(1.2)	-6.0(1.5)

Here a positive sign means that the wave number of the D_1 line for the indicated isotope is greater than that for ^{133}Cs.

The normal volume shift is calculated to be 10.7×10^{-3} cm^{-1} for the addition of one neutron. There is evidence that points to the cancellation of the normal volume effect by the deformation effect as a possible explanation of the smallness of the observed shifts.

I. INTRODUCTION

Of the methods currently available for the study of isotope shifts, none is generally suitable for the study of radioactive isotopes, especially short-lived ones. Conventional optical spectroscopy, level crossing spectroscopy, optical scanning methods, and other techniques where the light is detected are not suitable for studying trace amounts of radioactive isotopes in the presence of large amounts of stable carrier. Moreover, wall interaction interferes with attempts to study small quantities of separated isotopes.

It has been shown recently that the atomic beam method can be extended to the study of isotope shifts in radioactive isotopes. This method has the considerable advantage over any currently existing techniques that it can be applied to radioactive nuclei in the presence of large amounts of stable carrier.

In this thesis we report the measurement of isotope shifts on five radioactive cesium isotopes. These cesium isotopes are chosen as the subject of the study because of the availability of the methods for production and detection. In addition, a study of the isotope shifts over a large range of neutron number is of particular interest in order to observe the changes in the value of $\langle r^2 \rangle$ and in the nuclear shape from the spherical nuclei around ^{137}Cs (which has a magic number of 82 neutrons) to neutron deficient Cs isotopes where a region of deformed nuclei is expected.

II. THEORY OF ISOTOPE SHIFT

Isotope shifts refer to the displacement among the centers of gravity of the hfs patterns of the different isotopes of an element. The only nuclear properties which are now generally assumed to be of major importance in causing isotope shifts are the mass and the distribution of nuclear charge. Other effects, such as nuclear compressibility, nuclear polarization, etc., are omitted from the present discussion, since there is no evidence that they contribute appreciably to the observed isotope shifts, and they have not been treated theoretically in any detail.

As a reference level for the purpose of calculation, we consider the term energy appropriate to a point nucleus of infinite mass. For both mass and field effects, we adopt the following notation. The term energy of an actual nucleus differs from the reference term energy by an amount ΔE, and the change in ΔE from one isotope to another is $\delta(\Delta E)$. In general, δ will be used to indicate changes in a quantity between isotopes. In this section $\delta(\Delta E)$ will be called positive if the level of the lighter isotope lies lower than that of the heavier isotope. In order to find the shift in a spectral line, $\delta(\Delta E)$ must be evaluated for both the levels involved in the transition.

A. Nuclear Mass Effects

1. Normal Mass Effect

The non-relativistic Hamiltonian for a free atom with n electrons is of the form

$$\mathcal{H} = \frac{1}{2m} \sum_{j=1}^{n} \vec{p}_{oj}^{\,2} + \frac{1}{2M} \vec{P}_o^{\,2} + V(\vec{r}_{oj} - \vec{R}_o) \tag{1}$$

where $\vec{P}_o$ is the nuclear momentum and $\vec{p}_{oj}$ the electronic momenta relative to a fixed coordinate system. M and m are the nuclear and electronic masses, and V is the potential energy. The nuclear coordinate is designated $\vec{R}_o$ and the electronic coordinates $\vec{r}_{oj}$.

The following transformation leads to coordinates for the center of mass and electronic coordinates relative to the nucleus:

$$\vec{R} = \frac{M\vec{R}_o + \Sigma m \vec{r}_{oj}}{M + nm} \quad , \quad \vec{r}_j = \vec{r}_{oj} - \vec{R}_o \quad . \tag{2}$$

In terms of the new coordinates, the x-component of momentum of the center of mass is expressed as $P_x = i\hbar\partial/\partial x$. The quantities of $p_{jx} = i\hbar \frac{\partial}{\partial x_j}$ are the x-components of electronic momentum relative to the center of mass even though x_j is measured relative to the moving nucleus.

In a coordinate system where the center of mass is at rest ($\vec{P} = 0$), the Hamiltonian takes the form

$$\mathcal{H} = \frac{1}{2m} \Sigma_j \vec{p}_j^{\,2} + \frac{1}{2M} (\Sigma_j \vec{p}_j)^2 + V(\vec{r}_j) \quad . \tag{3}$$

Comparison with Eq. (1) leads to a simple interpretation of the terms in Eq. (3). The first term on the right-hand side of Eq. (3) is just the kinetic energy of the electrons ($\vec{p}_{oj} = \vec{p}_j$). The second term represents the recoil kinetic energy of the nucleus ($P_o = -\Sigma_j \vec{p}_j$).

It is convenient to expand the second term on the right-hand side of Eq. (3) and group the squared momenta with the first term:

$$\mathcal{H} = \frac{1}{2}\left(\frac{1}{m} + \frac{1}{M}\right) \sum_j \vec{p}_j^{\,2} + \frac{1}{2M} \sum_{j\neq k} \vec{p}_j \cdot \vec{p}_k + V. \tag{4}$$

The reduced mass is defined by $\frac{1}{\mu} = \frac{1}{m} + \frac{1}{M}$.

The first term on the right-hand side of Eq. (4) gives rise to the well-known normal mass effect. This is the only mass effect that occurs in hydrogen and one-electron ions.

To see the energy dependence upon μ, we consider the Schroedinger equation

$$\left[-\frac{\hbar^2}{2\mu} \sum_j \nabla_j^2 + V(\vec{r}_1, \ldots, \vec{r}_u) - E(\mu)\right] \psi = 0 \tag{5}$$

Let the $\vec{r}_j$ be formally replaced by $\vec{r}_j' = \left(\frac{\mu}{m}\right) \vec{r}_j$. The potential energy, if magnetic effects are ignored, scales inversely as a length

$$V = -\sum_j \frac{Ze^2}{r_j} + \sum_{j\neq k} \frac{e^2}{r_{jk}} \quad , \tag{6}$$

and hence

$$V(\vec{r}) = \frac{\mu}{m} V(\vec{r}') \quad . \tag{7}$$

The Schroedinger equation then becomes

$$\left[-\frac{\hbar^2}{2m} \nabla_j'^2 + V(\vec{r}') - \frac{m}{\mu} E(\mu)\right] \psi = 0 \quad . \tag{8}$$

This equation has the same form as Eq. (5), and thus the energy levels depend upon the reduced mass according to

$$\frac{E(\mu)}{E(m)} = \frac{\mu}{m} \quad .$$

Thus

$$\delta(\Delta E)_{\text{nor. mass}} = E(\mu)\frac{\delta\mu}{\mu} = E(\mu)\frac{\mu\delta M}{M^2} \quad . \tag{9}$$

2. Specific Mass Effect

The second term on the right-hand side of Eq. (4) gives rise to the so-called specific mass effect. Because of the presence of the nuclear mass in the denominator, this term is small in magnitude compared with the remainder of the Hamiltonian and may be treated as a perturbation. However, since it contains cross products of the momenta of different electrons, the specific mass effect is not susceptible of exact calculation, though in light elements results in moderate agreement with experiment have been obtained. For heavier elements many electrons are involved and the calculations become rapidly more complicated.

The differences in the mass effect for the isotopes of a given element is proportional to $1/M^2$, so that it is reasonable to expect that the order of magnitude of the specific mass effect decreases through the periodic table in the same way as the normal mass effect does. Kopfermann[1] suggests that starting from the rare earths, it is fairly safe to neglect mass effects entirely, in comparison with field effects.

B. Nuclear Field Effects

1. Nuclear Volume Effect

A system consisting of an electron and a point nucleus possesses a certain energy. If the electron has an appreciable probability density at radii down to zero, as in the case of an s-electron, then the energy of the system is higher if the nucleus is spread out, for instance over a sphere with radius r_o, than if it were concentrated at a point. Thus the nuclear electrostatic potential acting on the electron depends on the nuclear charge distribution; if this changes

from one isotope to another, the energy of an electron which penetrates the nucleus will also change in the two cases.

In the early work of Racah[2] and Rosenthal and Breit[3] the change in binding energy of an electron due to the difference in its electrostatic interaction with a point charge and the same charge spread over the nuclear volume is calculated using a perturbation method; with this the difference between two isotopes of the potential energy of the electron in the nuclear region is averaged over the relativistc charge density when the electron is moving in the field of a point nucleus. The poor agreement (the experimental isotope shift being in general smaller by a factor of 2-3[4]) of the experimental data with calculations based on the simple perturbation theory is not too surprising in view of the possibility that the spreading of the charge would strongly distort the wave function of the electron from its Coulomb form just inside the nuclear region, where the perturbation takes place, and thus considerably affect the isotope shift. Attempts to reduce this large discrepancy between the experimental data and the theory has resulted in the development of a more rigorous and accurate method which was founded by Broch[5] and later extended by Bodmer.[6] This method has the advantage not only of simplicity and directness but also of showing quite clearly what approximations are made in obtaining the final expression. Using this method and a value of $1.2\ A^{1/3}$ fm (instead of the old value of $1.5\ A^{1/3}$ fm) for the nuclear radius, the isotope shift is brought into considerably better agreement with the experimental data.

Consider the solutions to the radial Dirac equations for the electron (a) with the nuclear charge assumed concentrated at a point, and (b) with

an extended nuclear charge distribution. It is convenient to use the quantities

$$x = \frac{2Zr}{a_H} \quad , \; a = Z\alpha$$

$$\varepsilon = \frac{E}{mc^2} \quad , \; U(r) = \frac{V(r)}{mc^2}$$

where $a_H = \frac{\hbar^2}{me^2}$ is the Bohr radius and $\alpha = \frac{e^2}{\hbar c}$ the fine structure constant; V(r) is the potential energy (assumed spherically symmetric) of the electron in the field of the nuclear charge distribution. The radial Dirac equations may then be written in the form

$$\begin{aligned} \frac{df_k}{dx} &= \frac{k}{x} f_k + \frac{1}{2a} (1+U-\varepsilon) g_k \\ \frac{dg_k}{dx} &= \frac{k}{x} g_k + \frac{1}{2a} (1-U-\varepsilon) f_k \end{aligned} \tag{10}$$

where

$$\begin{aligned} k &= -(\ell+1) \qquad \text{for } j = \ell + 1/2 \\ &= \ell \qquad\quad\;\; \text{for } i = \ell - 1/2 \end{aligned}$$

is the Dirac quantum number of the electron, and f_k, g_k correspond to the small and large components of the Dirac wave function, respectively.

Quantities appropriate to the point nucleus case will be distinguished by a prime. Then from Eq. (10) and the corresponding equations for f'_k, g'_k we obtain

$$2a\, mc^2 \frac{d}{dx} (f_k g'_k - f'_k g_k) = (\Delta V - \Delta E)(f_k f'_k + g_k g'_k) \tag{11}$$

where $\Delta V = V - V'$ and $\Delta E = E - E' = \Delta E_{\text{spherical}}$. We consider a point x_1 corresponding to a distance of the order of nuclear dimensions and such that x_1 is outside the volume occupied by the extended nuclear charge

distribution, i.e. such that $\Delta V = 0$ for $x \geq x_1$. Then integrating Eq. (11) from $x = x_1$ to $x = \infty$, we obtain

$$\Delta E_{\text{spherical}} = 2a\, mc^2 (f_k g_k' + f_k' g_k)_{x = x_1} / N(x_1) \tag{12}$$

with

$$N(x_1) = \int_{x_1}^{\infty} (f_k f_k' + g_k g_k')\, dx \quad . \tag{13}$$

Using the normalization

$$\int_0^{\infty} (f_k^2 + g_k^2)\, dx = 1 \tag{14}$$

we may put $N(x_1) = 1$ to a good approximation, since $x_1 \approx \alpha^2 Z A^{1/3} << 1$, the corresponding relative error in $N(x_1)$, and hence $\Delta E_{\text{spherical}}$, being considerably less than x_1. Then

$$\Delta E_{\text{spherical}} = 2a\, mc^2 (f_k g_k' - f_k' g_k)_{x = x_1} \tag{15}$$

Denoting the regular and irregular Coulomb functions appropriate to a point charge Ze and an energy E by $aF_k^{(r)}$, $aF_k^{(i)}$, and $G_k^{(r)}$, $G_k^{(i)}$ for the small and large components respectively, we may write for $x \geq x_o$, where the potential is that due to a point charge,

$$\begin{aligned} f_a &= a\left(C_1 F_k^{(r)} + C_2 F_k^{(i)}\right) \\ g_k &= C_1 G_k^{(r)} + C_2 G_k^{(i)} \end{aligned} \qquad (x \geq x_1) \tag{16}$$

for a point nucleus $C_2 = 0$. Thus C_2/C_1 gives the amount of admixture of the irregular Coulomb solution due to the deviation of the charge distribution from a point charge. For x_1 corresponding to a distance of the order of nuclear radius the potential energy is very much larger in absolute value than the binding energy and it is a very good

approximation to neglect the latter in evaluating the functions F, G at the point x_1. These may then be expressed in terms of Bessel functions, namely

$$f_k(x) = a[C_1 J_{2\sigma}(2x^{1/2}) + C_2 J_{-2\sigma}(2x^{1/2})]$$
$$g_k(x) = C_1 A_{2\sigma}(2x^{1/2}) + C_2 A_{-2\sigma}(2x^{1/2}) \tag{17}$$

with

$$A_{2\sigma} = (k-\sigma)J_{2\sigma} + x^{1/2}J_{2\sigma+1}$$
$$A_{-2\sigma} = (k+\sigma)J_{-2\sigma} + x^{1/2}J_{-2\sigma-1}$$

where $\sigma = (k^2-a^2)^{1/2}$. Since $x_1 \ll 1$, it is in addition a very good approximation to retain only the lowest power of x_1 in the expansion of the Bessel functions and Eq. (15) can then be shown to become

$$\Delta E_{\text{spherical}} = -2a^2 C_1^2 \left(\frac{C_2}{C_1}\right) mc^2 \frac{1}{\Gamma(2\sigma)\Gamma(1-2\sigma)} x_1^{2\sigma} \tag{18}$$

where Γ denotes the gamma functions. Only the ratio C_2/C_1 on the right-hand side of Eq. (18) depends on the nuclear charge distribution. Putting $K_k = f_k/g_k$, we obtain from Eq. (17)

$$\frac{C_2}{C_1} = \frac{aJ_{2\sigma}(2x_1^{1/2}) - K_k(x_1)A_{2\sigma}(2x_1^{1/2})}{K_k(x_1)A_{-2\sigma}(2x_1^{1/2}) - aJ_{-2\sigma}(2x_1^{1/2})} \tag{19}$$

where $K_k(x_1)$ is now assumed evaluated neglecting the binding energy and is determined from the solution interior to x_1 of the Ricatti equation

$$\frac{dK_k}{dx} = \frac{2k}{x}K_k + \frac{U-2}{2a}K_k^2 + \frac{U}{2a} \qquad x \le x_1 \tag{20}$$

which is obtained from Eq. (10) by differentiating K_k with respect to x and setting $\varepsilon = 1$. If we rewrite Eq. (20) in the form

$$\frac{U}{2a} + \frac{U-2}{2a} K_k^2 = \frac{dK_k}{dx} - \frac{2k}{x} K_k$$

this may be transformed into an integral equation by multiplying by the integrating factor x^{-2k},

$$K_k(x) = x^{2k} \int_o^x \left(\frac{U}{2a} + \frac{U-2}{2a} K_k^2\right) x'^{-2k} \, dx' \tag{21}$$

where $k < 0$. If $K_k << 1$, this may be solved by successive iteration starting with $K_k = 0$.

Expanding the Bessel functions and keeping only the lowest power of x_1, Eq. (19) becomes

$$\frac{C_2}{C_1} = \frac{\Gamma(1-2\sigma)}{\Gamma(1+2\sigma)} \frac{a-(k-\sigma)K_k(x_1)}{a-(k+\sigma)K_k(x_1)} \quad . \tag{22}$$

As is evident from the derivation, C_2/C_1 is then independent of x_1. Substituting Eq. (22) in Eq. (18), we have

$$\Delta E_{\text{spherical}} = 2a^2 C_1^2 mc^2 \frac{1}{2\sigma\Gamma^2(2\sigma)} \frac{a-(k-\sigma)K_k(x_1)}{a-(k+\sigma)K_k(x_1)} x_1^{2\sigma} \quad . \tag{23}$$

The value of $K_k(x_1)$ depends on the nuclear charge distribution. The isotope shift is then

$$\delta(\Delta E)_{\text{spherical}} = 2a^2 C_1^2 mc^2 \frac{1}{\Gamma^2(2\sigma)} \frac{a\delta K_k(x_1)}{[a-(k+\sigma)K_k(x_1)]^2} x_1^{2\sigma} \quad . \tag{24}$$

If in the nuclear region it is permissible to write U/2a instead of (U-2)/2a for the factor multiplying K_k^2, Eq. (20) becomes

$$\frac{dK_k}{dx} = \frac{2k}{x} K_k + \frac{U}{2a} (1+K_k^2) \quad . \tag{25}$$

This approximation is equivalent to assuming $x_1/a^2 << 1$ for the factor multiplying K_k^2 and is somewhat more stringent, especially for lighter elements, than the condition $x_1 << 1$ assumed previously. However, for $k < 0$ we see from the iteration procedure for obtaining K_k that the term neglected only affects K_k in the second iteration, the error involved in the additional term due to this being less than 10%. The only practically important case for the isotope shift is in fact that of an s electron, $k = -1$, and since, as we shall see, the additional term due to the second iteration makes only a relatively small contribution, the error in K due to this approximation is very small. In what follows we shall consider only s electrons and write K_{-1} simply as K.

Consider the spherically symmetric potential energy of the type

$$\left.\begin{aligned} V &= \frac{n+1}{n} \left[1 - \frac{1}{n+1} \left(\frac{r}{r_o}\right)^n\right] \frac{Ze^2}{r_o} \quad , \quad r < r_o \ ; \\ V &= -\frac{Ze^2}{r} \quad , \qquad\qquad\qquad r > r_o \end{aligned}\right\} \tag{26}$$

where r_o can be considered as the nuclear radius. n can vary from -1 for a point charge through n = 2 for a uniform charge distribution to $n = \infty$ when all the charge is on the surface. For potentials of this form it is then seen by rewriting Eq. (25) that

$$K = K\left(\frac{x}{x_o}\right) \tag{27}$$

where $x_o = \frac{2Zr_o}{a_H}$. From this it follows that

$$\frac{\partial K(x_1)}{\partial x_o} = - \frac{x_1}{x_o} \frac{\partial K(x_1)}{\partial x_1}$$

and therefore, using Eq. (25),

$$\frac{\partial K(x_1)}{\partial x_o} = - \frac{x_1}{x_o} \left\{ - \frac{2K(x_1)}{x_1} + \frac{U}{2a} [1+K^2(x_1)] \right\} \quad . \tag{28}$$

With x_1 outside the nuclear charge distribution where $U = -\frac{2a^2}{x_1}$,

$$\frac{\partial K(x_1)}{\partial x_o} = \frac{1}{x_o} \{a[1+K^2(x_1)] + 2K(x_1)\}$$

$$= \frac{1}{ax_o} [a+(1+\sigma)K(x_1)][a+(1-\sigma)K(x_1)] \quad . \tag{29}$$

Substituting $\delta K(x_1) = \frac{\partial K(x_1)}{\partial x_o} \delta x_o$ in Eq. (24), we obtain

$$\delta(\Delta E)_{\text{spherical}} = 2a^2 C_1^2 mc^2 \frac{1}{\Gamma^2(2\sigma)} \frac{a+(1+\sigma)K(x_1)}{a+(1-\sigma)K(x_1)} x_1^{2\sigma} \frac{\delta x_o}{x_o} \quad . \tag{30}$$

Recalling that the only condition on x_1 is that x_1 be outside the nuclear charge distribution and of the order of nuclear dimensions, we may set $x_1 = x_o$ in the above equation, obtaining

$$\delta(\Delta E)_{\text{spherical}} = 2a^2 C_1^2 mc^2 \frac{1}{\Gamma^2(2\sigma)} \frac{a+(1+\sigma)K(x_o)}{a+(1-\sigma)K(x_o)} x_o^{2\sigma} \frac{\delta x_o}{x_o} \quad . \tag{31}$$

Assuming the validity of Eq. (25) for k = -1, we may write Eq. (21) as

$$K(x) = \frac{1}{x^2} \int_o^x \frac{U}{2a} [1+K^2(x')] x'^2 \, dx' \quad . \tag{32}$$

For the first iteration we have

$$K^{(1)}(x) = \frac{1}{2ax^2} \int_o^x U x'^2 \, dx' \tag{33}$$

and for the second

$$K^{(2)}(x) = K_o^{(1)}(x) + \frac{1}{2ax^2} \int_o^x U\left[K^{(1)}(x')\right]^2 x'^2\, dx' \quad . \tag{34}$$

Using this iteration process $K(x_o)$ can be found as a power series in a. Specifically for a uniform charge distribution we have

$$K^{(2)}(x_o) = K(a) = -\frac{2a}{5}(1+0.105a^2) \quad . \tag{35}$$

For the potential [Eq. (26)] the isotope shift then depends on the radius x_o only through $x_o^{2\sigma}$ in addition to the relative change of radius $\delta x_o/x_o$.

Although it would appear from the above that the first iteration is not a very good approximation for $K(x_o)$, nevertheless as far as the equivalence of two charge distributions is concerned it is sufficient to use only the first iteration. By integrating by parts twice and using Poisson's equation, the integral in Eq. (33) may be expressed in terms of an integral over the charge density ρ, i.e.

$$\int_o^r Vr'^2\, dr' = \frac{2\pi}{3}\int_o^\infty e\rho r'^4\, dr' - \frac{Ze^2r^2}{2} \tag{36}$$

The upper limit in the integral on the right is actually r but may be replaced by ∞, since for the calculation of K(x) r must be effectively outside the charge distribution and for the potential [Eq. (26)] ρ has the form

$$\left.\begin{aligned} \rho &= \frac{n+1}{4\pi}\,\frac{Ze}{r_o^3}\left(\frac{r}{r_o}\right)^{n-2}, \qquad r < r_o \\ \rho &= 0, \qquad r > r_o \quad . \end{aligned}\right\} \tag{37}$$

Now let us look at the relation between the equivalent radii, R_s and R_u, of a surface and a uniform charge distribution, respectively, which give the same $K(x_o)$, by equating the expressions (34) for $n = 2$ and $n = \infty$ with $x = x_u$,

$$\left(\frac{R_s}{R_u}\right)^2 = \frac{3}{5}\,(1-0.012a^2) \quad . \tag{38}$$

The first term is due to the first iteration and can immediately be obtained by equating

$$\int_o^\infty \rho r^4 dr = \frac{Ze}{4\pi}\,\frac{n+1}{n+3}\,r_o^{\,2} \tag{39}$$

for $n = 2$ and $n = \infty$. The term from the second iteration makes only a very small contribution. Thus the use of the first iteration is a very good approximation when the equivalence between the two charge distributions and not the actual value of $K(x_o)$ is being considered. Since the difference between a uniform and a surface charge distribution can be considered as a extreme, the magnitude of the term in Eq. (38) due to the second iteration may be regarded as in the nature of an upper limit to such a term in the expression for the radius of the uniform charge distribution equivalent to some actual distribution. We see then that for any charge distribution ρ, the radius of the equivalent uniform charge distribution will be given with good accuracy by

$$R_u^{\,2} = \frac{5}{3}\,\frac{4\pi}{Ze}\int_o^\infty \rho r^4 dr = \frac{5}{3}\langle r^2\rangle \quad . \tag{40}$$

From Eqs. (39) and (40) it follows that

$$\frac{\delta R_u}{R_u} = \frac{\delta r_o}{r_o} \quad .$$

Then the volume dependent isotope shift can be expressed in terms of R_u as

$$\delta(\Delta E)_{\text{spherical}} = 4a^2 C_1^2 mc^2 \frac{1}{2\Gamma^2(2\sigma)} \frac{a+(1+\sigma)K(a)}{a+(1-\sigma)K(a)} x_u^{2\sigma} \frac{\delta R_u}{R_u} \quad . \tag{41}$$

In this way we have related the isotope shift to the root-mean-square radius of the nuclear charge distribution, which can be obtained from such experiments as the electron scattering, x-ray spectroscopy of muonic atoms, etc. The value of K(a) in Eq. (41) is that appropriate for a uniform charge distribution and is given by Eq. (35). C_1^2 is determined from the normalization of the radial Dirac wave function by putting g_k/r asymptotically equal to the radial Schroedinger wave function for large r. It has been shown by Rosenthal and Breit[3] that for an s electron

$$C_1^2 = \frac{\pi R_\infty}{Z^3 e^2} a_H^4 \, |\psi(0)|^2 \tag{42}$$

where R_∞ is the Rydberg constant and $\psi(0)$ is the value of the Schroedinger wave function at the origin. The value of $|\psi(0)|^2$ can be obtained from optical spectroscopic data by means of the semi-empirical Fermi-Segrè formula[7]

$$|\psi(0)|^2 = \frac{Z_i Z_o^2}{\pi a_H^3 (n^*)^3} \left(1 - \frac{d\Delta}{dn}\right) , \tag{43}$$

where Z_i is the internal effective nuclear charge, usually taken as Z; Z_o is the external atomic charge felt by the valence electron; $n^* = n-\Delta$ is the effective quantum number obtained by equating the term value energy to $-R_\infty Z_o^2/(n^*)^2$, and n is the principal quantum number while Δ is the quantum defect. An alternative method for determining $|\psi(0)|^2$ is the comparison of the atomic hfs constant A with the known nuclear moment, using the relation in Eq. (73).

2. Nuclear Deformation Effect

Nuclei which are deformed to a non-spherical shape will, after averaging over all orientations, appear more extended radially than spherical nuclei of the same volume, thus giving rise to a change in R_u; if the shape changes as neutrons are added, this again will alter R_u. This effect was introduced into the theory by Brix and Kopfermann[8] in an attempt to account for the observed isotope shift of Nd, Sm, and Eu. The theory has been considered explicitly by Ford[9] and by Wilets et al.,[10] and independently by Bodmer.[11]

For the consideration of the nuclear deformation a quadrupole deformation is generally assumed. In this case the surface of the nucleus can be represented by

$$R(\theta) = a_o \left[1+\alpha P_2 (\cos\theta)\right] \tag{44}$$

where $P_2 (\cos\theta) = 1/2(3\cos^2\theta - 1)$ and α is related to the Bohr deformation parameter β by the relationship $\alpha^2 = \frac{5}{4\pi}\beta^2$. In order to isolate the deformation effect from other effects, it is further assumed that the nucleus has constant volume $\frac{4\pi}{3} R_o^3$ and uniform density

$$\begin{aligned} \rho &= \frac{3Ze}{4\pi R_o^3} \quad , \quad r < R(\theta) \\ \rho &= 0 \quad , \quad r > R(\theta) \ . \end{aligned} \tag{45}$$

The constant volume assumption relates the parameter a_o and R_o appearing in Eq. (44) and Eq. (45), according to

$$a_o = R_o \left[1+(3/5)\alpha^2+(2/35)\alpha^3\right]^{-1/3} \ . \tag{46}$$

Then for the deformed distribution we obtain from Eq. (40)

$$R_u^2 = \frac{5}{3}\frac{1}{Ze}\int \rho r^2 d\vec{r}$$

$$= \frac{a_o^5}{2R_o^3}\int_{-1}^{1}[1+\alpha P_2(\cos\theta)]^5\, d(\cos\theta)\ . \tag{47}$$

Since α^2 is usually very small compared with unity, the above expression can accuratley be approximated by

$$R_u^2 = R_o^2(1-\alpha^2+\cdots)(1+2\alpha^2+\cdots)$$

$$= R_o^2(1+\alpha^2+\cdots)\ . \tag{48}$$

Hence we have the approximate result

$$R_u = R_o(1+\tfrac{1}{2}\alpha^2)\ . \tag{49}$$

Substituting Eq. (49) in (23), the resulting expression then contains the information on both field effects and may be called ΔE_{field}. Expanding $(1+\frac{1}{2}\alpha^2)^{2\sigma}$ and keeping terms up to α^2, we may write

$$R_u^{2\sigma} = R_o^{2\sigma}\,(1+\sigma\alpha^2), \tag{50}$$

obtaining

$$\Delta E_{field} = \Delta E_{spherical}(1+\sigma\alpha^2) = \Delta E_{spherical} + \Delta E_{deformation} \tag{51}$$

Thus

$$\delta(\Delta E)_{field} = \delta(\Delta E)_{spherical} + \delta(\Delta E)_{deformation}$$

$$= \Delta E_{spherical} \; 2\sigma \frac{\delta R_o}{R_o} + \sigma\delta(\alpha^2) \tag{52}$$

$$= \pi R_\infty \frac{a_H^3}{Z} \; |\psi(0)|^2 \frac{1}{\sigma\Gamma^2(2\sigma)} \frac{a+(1+\sigma)K(a)}{a+(1-\sigma)K(a)} x_o^{2\sigma} \; 2\sigma \frac{\delta R_o}{R_o} + \sigma\delta(\alpha^2)$$

It is seen that $\delta(\Delta E)_{field}$ can be expressed as a sum of two terms, one depending on changes in nuclear volume and one depending on changes in nuclear shape. $\Delta E_{deformation}$ is always very much smaller than $\Delta E_{spherical}$, but $\delta(\Delta E)_{deformation}$ may be of the same order of magnitude as $\delta(\Delta E)_{spherical}$ since the nuclear deformation may change by a large fraction of itself from one isotope to another.

From a consideration of electron scattering results for about twenty nuclei, the deformations of which are known to be small, Elton[12] has given a semi-empirical formula for R_o,

$$R_o = 1.123A^{1/3} + 2.352A^{-1/3} - 2.070A^{-1} \text{ fm.} \tag{53}$$

The expression now universally adopted is $R_o = 1.2A^{1/3}$ fm.

III. HYPERFINE STRUCTURE

If the finite extension of the nucleus is taken into account, the electrostatic interaction between an electron and the nucleus must be expressed as an integral of volume elements of the electron and the nucleus, i.e.

$$\langle \mathcal{H}_E \rangle = \int_{\tau_e} \int_{\tau_n} \frac{\rho_e \rho_n}{|\vec{r}_e - \vec{r}_n|} \, d\tau_e d\tau_n \tag{54}$$

where ρ_e is the electronic charge density and ρ_n the nuclear charge density. Assuming $r_e > r_n$, we may expand $1/|\vec{r}_e - \vec{r}_n|$ in terms of Legendre polynomials and use the spherical harmonic addition theorem to obtain

$$\langle \mathcal{H}_E \rangle = \sum_k \sum_q (-1)^q \left[\int_{\tau_e} \left(\frac{4\pi}{2k+1}\right)^{\frac{1}{2}} \frac{\rho_e}{r_e^{k+1}} Y_{-q}^{(k)} (\theta_e, \phi_e) \, d\tau_e \right] \times \left[\int_{\tau_n} \left(\frac{4\pi}{2k+1}\right)^{\frac{1}{2}} \rho_n r_n^k Y_q^{(k)} (\theta_n, \phi_n) \, d\tau_n \right] , \tag{55}$$

or

$$\mathcal{H}_E = \sum_k \overleftrightarrow{Q}^{(k)}(e) \cdot \overleftrightarrow{F}^{(k)}(n) \quad . \tag{56}$$

The terms $\overleftrightarrow{Q}^{(k)}$ and $\overleftrightarrow{F}^{(k)}$ are spherical tensor operators of rank k operating on the electronic and nuclear coordinates, respectively. It is evident from Eqs. (55) and (56) that they are given by

$$Q_q^{(k)} = - \left(\frac{4\pi}{2k+1}\right)^{\frac{1}{2}} \frac{e}{r_e^{k+1}} Y_q^{(k)} (\theta_e, \phi_e) \tag{57a}$$

and

$$F_q^{(k)} = \left(\frac{4\pi}{2k+1}\right)^{\frac{1}{2}} e r_n^k Y_q^{(k)} (\theta_n, \phi_n) \quad . \tag{57b}$$

Restricting consideration to stationary nuclear and electronic current distributions, for which $\vec{\nabla}\cdot\vec{j} = 0$, we may write

$$\vec{j}_n = c\,\vec{\nabla} \times \vec{m}_n \tag{58a}$$

and

$$\vec{j}_e = c\,\vec{\nabla} \times \vec{m}_e \ . \tag{58b}$$

Here $\vec{m}_e$ and $\vec{m}_n$ are, like the magnetic field intensity H, pseudovectors. Ramsey[13] has shown that under these conditions the magnetic interaction

$$\langle \mathcal{H}_M \rangle = -\frac{1}{c} \int_{\tau_n} \vec{j}_n \cdot \vec{A}_e \, d_n = -\frac{1}{c} \int_{\tau_e} \vec{j}_e \cdot \vec{A}_n d\tau_e$$

can be written as

$$\langle \mathcal{H}_M \rangle = \int_{\tau_e} \int_{\tau_n} \frac{(-\vec{\nabla}_e \cdot \vec{m}_e)(-\vec{\nabla}_n \cdot \vec{m}_n)}{|\vec{r}_e - \vec{r}_n|} \, d\tau_e \, d\tau_n \ . \tag{59}$$

Since this has the same form as Eq. (54) we obtain at once

$$\mathcal{H}_M = \sum_k \overleftrightarrow{M}^{(k)}(e) \cdot \overleftrightarrow{N}^{(k)}(n) \tag{60}$$

where

$$M_q^{(k)} = -\left(\frac{4\pi}{2k+1}\right)^{\frac{1}{2}} \frac{\vec{\nabla}_e \cdot \vec{m}_e}{r_e^{\,k+1}} Y_q^{(k)}(\theta_e, \phi_e) \tag{61a}$$

and

$$N_q^{(k)} = -\left(\frac{4\pi}{2k+1}\right)^{\frac{1}{2}} (\vec{\nabla}_n \cdot \vec{m}_n) \, r_n^{\,k} \, Y_q^{(k)}(\theta_n, \phi_n) \ . \tag{61b}$$

Matrix elements of operators having the form of Eqs. (56) and (60) are easily taken in a representation where I and J couple to F [$(IJFM_F)$ representation]:

$$\sum_k \langle IJFM_F|\overleftrightarrow{Q}^{(k)}\cdot\overleftrightarrow{F}^{(k)}|I'J'F'M_F'\rangle = \sum_k (-1)^{I'+J+F}\delta_{FF'}\delta_{M_FM_F'} \times\begin{Bmatrix} I & J & F \\ J' & I' & k \end{Bmatrix}\langle J\|Q^{(k)}\|J'\rangle\langle I\|F^{(k)}\|I'\rangle \quad . \quad (62)$$

The 6-j symbol shows that the series breaks off for either $J + J' < k$ or $I + I' < k$.

The expectation value $\langle\psi|O|\psi\rangle$ of any operator O must have positive parity, since integrals over all space cannot depend on axis inversion. For states with well-defined parity, $|\psi|^2$ has positive parity; O must therefore have positive parity for $\langle\psi|O|\psi\rangle$ to be non-zero. Operators $Q^{(k)}$ and $F^{(k)}$ both have the parity of $Y^{(k)}$, i.e. $(-1)^k$. Therefore, only k even values are allowed in the electric case. Since $\vec{m}_e$ ($\vec{m}_n$) is a pseudovector, $\vec{\nabla}\cdot\vec{m}_e$ ($\vec{\nabla}\cdot\vec{m}_n$) is a pseudoscalar having parity -1, and $M^{(k)}$ and $N^{(k)}$ have the parity $(-1)Y^{(k)}$, or $(-1)^{k+1}$. Therefore, only k odd values are allowed in the magnetic case.

The first allowed electric interaction is $Q^{(o)}\cdot F^{(o)}$, which is just the Coulomb term. The second allowed term is $Q^{(2)}\ F^{(2)}$, the electric quadrupole term. Defining

$$Q = (\tfrac{2}{e})\langle II|Q_o^{(2)}|II\rangle \quad (63a)$$

$$q_J = -(\tfrac{2}{e})\langle JJ|F_o^{(2)}|JJ\rangle \quad (63b)$$

and using Eq. (62) we obtain

$$\langle IJFM_F | \overleftrightarrow{Q}^{(2)} \overleftrightarrow{F}^{(2)} | IJFM_F \rangle = \frac{-e^2 q_J Q[3K(K+1) - 4I(I+1)J(J+1)]}{8IJ(2I-1)(2J-1)} \tag{64}$$

where $K = F(F+1) - I(I+1) - J(J+1)$. The term Q is the nuclear quadrupole moment, and q_J is the gradient of the z-component of the electric field at the origin. The quantity $-e^2 q_J Q$ is called the electric quadrupole interaction constant and written as B.

The first allowed magnetic interaction is $\overleftrightarrow{M}^{(1)} \cdot \overleftrightarrow{N}^{(1)}$. Consideration of the classical interpretation of $M^{(1)}$ and $N^{(1)}$ shows that

$$\langle JJ | M_o^{(1)} | JJ \rangle = -\int_{\tau_e} \frac{\vec{\nabla}_e \cdot \vec{m}_e \cos\theta_e}{r_e^2} d\tau_e$$

$$= -\frac{1}{c} \int_{\tau_e} \frac{(\vec{j}_e \times \vec{r}_e)_z}{r_e^3} d\tau_e$$

$$= -\langle B_z \rangle_{JJ} \quad , \tag{65}$$

and

$$\langle II | N_o^{(1)} | II \rangle = -\int_{\tau_n} r_n (\vec{\nabla}_n \cdot \vec{m}_n) d\tau_n$$

$$= -\frac{1}{2c} \int_{\tau_n} (\vec{r}_n \times \vec{j}_n)_z d\tau_n$$

$$= (\mu_I)_z \quad . \tag{66}$$

Using Eqs. (62), (65), and (66) we can then write

$$\langle IJFM_F | M^{(1)} \cdot N^{(1)} | IJFM_F \rangle = -\frac{\mu_I \langle B_z \rangle_{JJ}}{IJ} \vec{I} \cdot \vec{J} \quad , \tag{67}$$

which serves to define the magnetic dipole interaction constant A as

$$A = - \frac{\mu_I \langle B_z \rangle_{JJ}}{IJ} \quad . \tag{68}$$

The classical expression for the magnetic field at the nucleus due to a circulating electron with permanent magnetic dipole moment is

$$\vec{B}(o) = - \frac{e}{c} \frac{\vec{r} \times \vec{v}}{r^3} - \frac{\mu(\vec{r} \cdot \vec{r}) - 3\vec{r}(\vec{\mu} \cdot \vec{r})}{r^5} \quad . \tag{69}$$

Writing that $m\vec{r} \times \vec{v} = \hbar \vec{\ell}$ and $\vec{\mu} = -2\mu_o \vec{s}$, the transition to the quantum mechanical form of this operator is made,

$$\vec{B}(o) = - \frac{2\mu_o}{r^3} \left(\vec{\ell} - \vec{s} + \frac{3\vec{s} \cdot \vec{r}}{r^2} \vec{r} \right) \quad . \tag{70}$$

This operator can be further simplified into[14]

$$\vec{B}(o) = - \frac{2\mu_o}{r^3} \left[\vec{\ell} - (10)^{\frac{1}{2}} (sC^{(2)})^{(1)} \right]$$

$$= - \frac{2\mu_o}{r^3} \vec{N} \quad . \tag{71}$$

For the case of one valence electron in a non-s state it can easily be shown that

$$\langle B(o) \rangle_{JJ} = -2\mu_o \left\langle \frac{1}{r^3} \right\rangle \frac{\ell(\ell+1)}{J+1} \quad . \tag{72}$$

So far we have restricted ourselves to the case of $r_e > r_n$; however, s electrons have a non-vanishing density at the origin and thereby violate this restriction. This density at the origin does not affect the electric quadrupole moment, since s electrons have spherically symmetric densities and therefore cannot contribute to the quadrupole interaction.

Fermi[15] has shown that there is a contact interaction between the intrinsic spin magnetic moment and the nuclear magnetic moment. Treating the electron as a relativistic particle obeying the Dirac equation and the nucleus as a point dipole, Fermi was able to obtain

$$A_s = \frac{16\pi}{3} g_I \mu_o^2 |\psi(o)|^2 \tag{73}$$

where $\psi(o)$ is the value of the Schroedinger wave function at the origin.

Because of the vanishing smallness of the contributions from the magnetic octupole moment and higher order electric and magnetic multipole moments, the hyperfine Hamiltonian is generally taken as

$$\mathcal{H}_{hfs} = \mathcal{H}_{M1} + \mathcal{H}_{E2} \ . \tag{74}$$

This Hamiltonian does not commute with either J or I, but does with their vector sum F. The (2J+1) degenerate fine structure levels are therefore split into 2I+1 or 2J+1 (whichever number is smaller) levels by the hyperfine structure interaction. The new levels are 2F+1 degenerate in the absence of an external magnetic field.

The interaction of the atom with an external magnetic field is given by

$$\mathcal{H}_{ext} = -g_J \mu_o \vec{J}\cdot\vec{H} - g_I \mu_o \vec{I}\cdot\vec{H} \ . \tag{75}$$

This term does not commute with F, but F is an approximately good quantum number at low fields. Therefore, at low fields the effect of the external magnetic field is to remove the (2F+1)-fold degeneracy of the eigenvalues through the interaction

$$\langle IJFM_F|\mathcal{H}_{ext}|IJFM_F\rangle = -g_F \mu_o H M_F \tag{76}$$

where

$$g_F = g_J \frac{F(F+1)+J(J+1)-I(I+1)}{2F(F+1)} + g_I \frac{F(F+1)+I(I+1)-J(J+1)}{2F(F+1)} .$$

In the high-field region (nuclear Paschen-Bach), F is no longer a good quantum number and eigenstates are best labeled by I, M_I; J, M_J.

IV. EXPERIMENTAL METHOD AND APPARATUS

A. Stark Effect

Experimentally, the isotope shifts have almost exclusively been measured by conventional optical methods. In 1965 Marrus and McColm[16] developed a new atomic beam method for the study of the Stark effect in optical transitions. In the present work this method was employed to study the isotope shifts in six cesium isotopes.

The perturbation of an energy level by an external electric field E is described, if the polarization of the nucleus is neglected, by the Hamiltonian

$$\mathcal{H}_{st} = -\vec{p} \cdot \vec{E} \tag{77}$$

where $\vec{p}$ is the induced dipole moment and is given by $\vec{p} = -e \sum_i \vec{r}_i$, $\vec{r}_i$ being the position vector of the i^{th} electron. Applying to an alkali for which we neglect perturbation of electrons in closed shells, then $\vec{p} = -e\vec{r}$, $\vec{r}$ being the position vector of the valence electron. It is well known that for states of well-defined parity the Hamiltonian $\mathcal{H}_{st}$ gives no first order effect. The second order perturbation gives for a state ψ_o characterized by the quantum numbers $(n^2L_JFM_F)$

$$\Delta W = \sum_{\psi} \frac{|\langle \psi_o | e\vec{r}\cdot\vec{E} | \psi \rangle|^2}{\Delta E(\psi, \psi_o)} \quad . \tag{78}$$

Neglecting the hyperfine energy of the states ψ in the denominator of Eq. (78), Marrus, McColm, and Yellin[17] have shown for an electric field directed along the z-axis that ΔW is independent of the quantum numbers F and M_F, and obtained for the states $^2S_{1/2}$ and $^2P_{1/2}$

$$\Delta W(n^2S_{1/2}) = \frac{1}{9}\ e^2E^2 \sum_{n'} \left\{ \frac{\left|\langle n'^2P_{1/2}\|r\|n^2S_{1/2}\rangle\right|^2}{\Delta E(n'^2P_{1/2},\ n^2S_{1/2})} \right.$$

$$\left. + \frac{2\left|\langle n\ ^2P_{3/2}\|r\|n^2S_{1/2}\rangle\right|^2}{\Delta E(n'^2P_{3/2},\ n^2S_{1/2})} \right\} \tag{79}$$

and

$$\Delta W(n^2P_{1/2}) = \frac{1}{9}\ e^2E^2 \sum_{n'} \left\{ \frac{\left|\langle n\ ^2S_{1/2}\|r\|n^2P_{1/2}\rangle\right|^2}{\Delta E(n'^2S_{1/2},\ n^2P_{1/2})} \right.$$

$$\left. + \frac{2\left|\langle n'^2D_{3/2}\|\ \|n^2P_{1/2}\rangle\right|^2}{\Delta E(n'^2D_{3/2},\ n^2P_{1/2})} \right\} \tag{80}$$

respectively.

The Stark shift can also be expressed in terms of the polarizability (α) of the state according to the usual relation

$$\Delta W(n^2L_Jm_J) = -\frac{E^2}{2}\,\alpha(n^2L_Jm_J). \tag{81}$$

Using the method of Bates and Damgard, Marrus et al. obtained from Eqs. (79) and (80) the following numerical values for $^2S_{1/2}$ and $^2P_{1/2}$

$$\alpha(6\ ^2S_{1/2}\ \pm 1/2) = 56 \times 10^{-24}\ \text{cm}^3$$

and

$$\alpha(6\ ^2P_{1/2}\ \pm 1/2) = 192 \times 10^{-24}\ \text{cm}^3\ .$$

Thus the Stark shift in the D_1 ($6\ ^2P_{1/2} \rightarrow 6\ ^2S_{1/2}$) line is given by

$$\delta(\Delta W) = -\frac{E^2}{2} \times 136 \times 10^{-24}\ . \tag{82}$$

Here the minus sign means a decrease of the transition frequency in the presence of an external electric field.

It should be noted that since α is independent of the sign of m_J the two components of the hyperfine doublet are shifted by the same amount, i.e., the hyperfine separation of the states $^2P_{1/2}$ and $^2S_{1/2}$ is not affected by a Stark field.

B. Apparatus

The apparatus employed is a conventional atomic beam machine with flop-in magnet geometry[18], as shown schematically in Fig. 1. In this machine the two regions, A and B, of very large inhomogeneous magnetic field have their field gradients in the same direction. In these two regions, the atoms are acted on by a force given by

$$F_z = - \frac{\partial \mathcal{H}_{ext}}{\partial z} \approx g_J \mu_o m_J \frac{\partial H}{\partial z} \quad . \tag{83}$$

This relation is obtained by evaluating $\mathcal{H}_{ext}$ as defined in Eq. (75) in the Paschen-Back region and neglecting the term in g_I, which is about 1/2000 of g_J. In order to be detected, an atom must have its deflection in the A region cancelled by its deflection in the B region; this cancellation can occur if

$$m_J(A) = -m_J(B) \quad .$$

This condition requires that the atom undergo a transition in the C region. The C region consists of a pair of electric field plates, with a gap of about 0.029 in. The plates consist of a heated-glass cathode and a stainless-steel anode (see Figs. 2 and 3), both of which are ground to within 10^{-4} in. The homogeneity of the electric field produced is estimated to be about 0.5% and is sufficiently good so that it does not

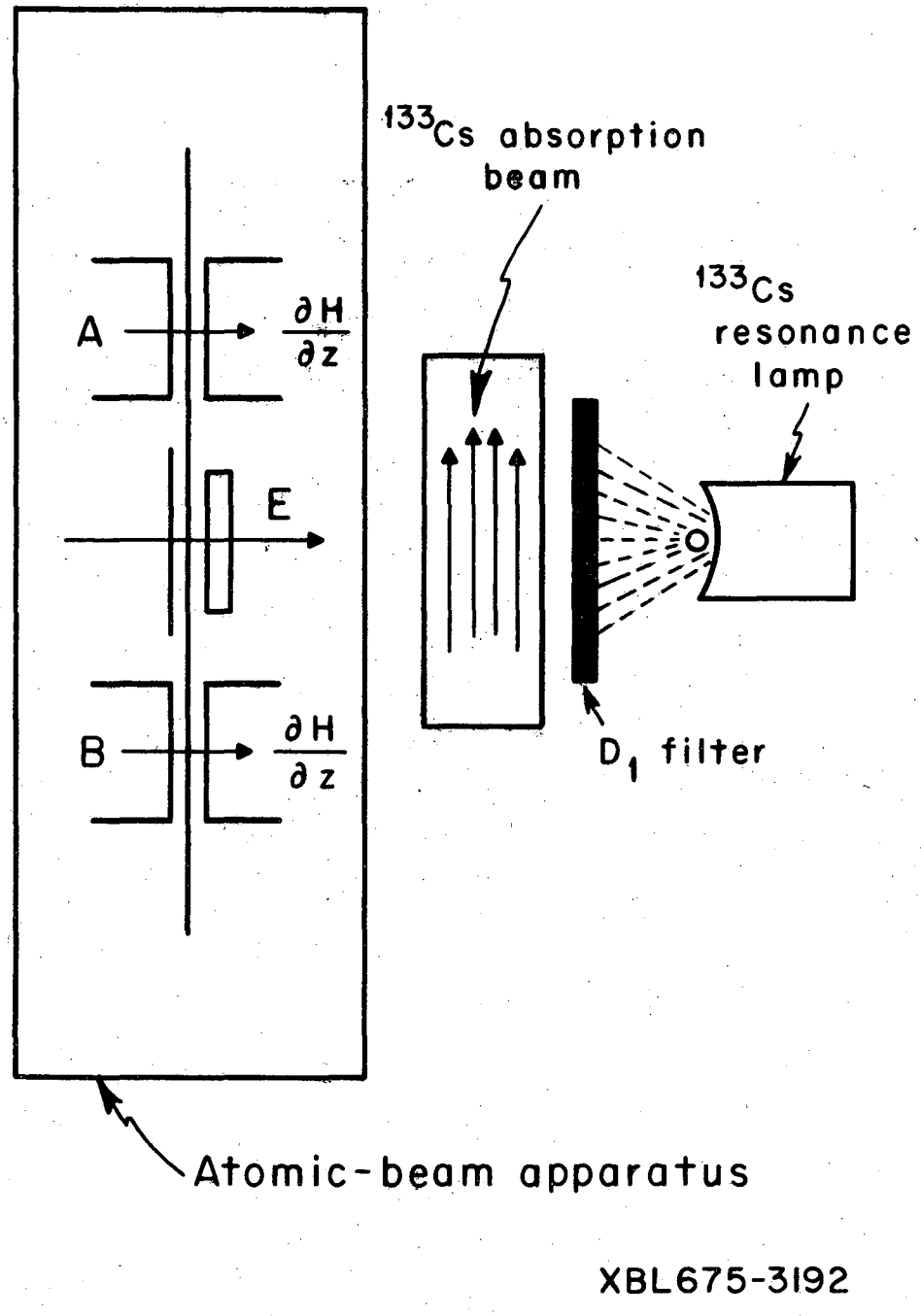

Fig. 1. Schematic diagram of apparatus.

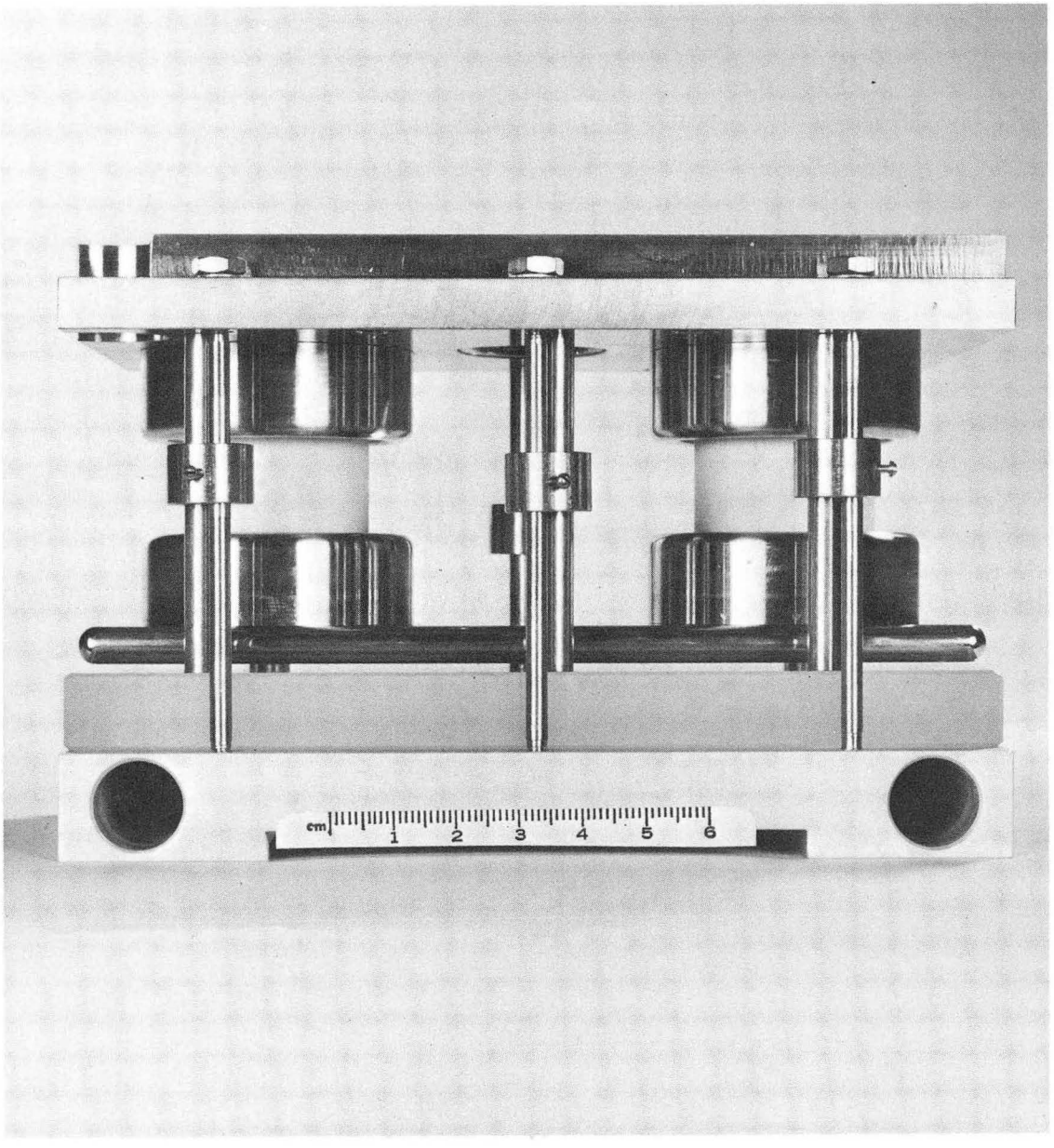

XBB 685-3070

Fig. 2. Assembled electric field plates, with 0.029 in. gap clearly shown.

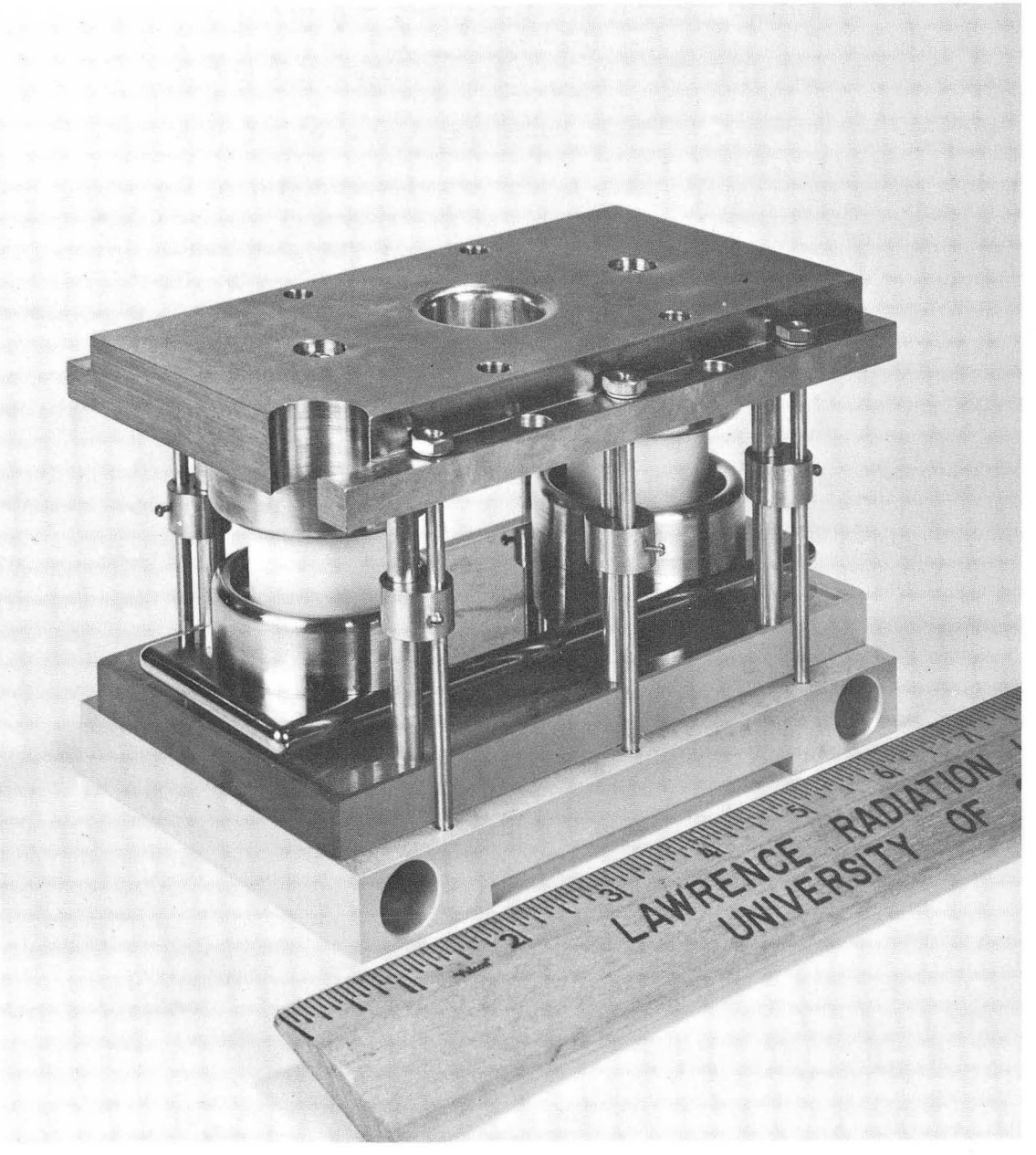

XBB 685-3071

Fig. 3. Another view of the electric field plates assembly.

contribute appreciably to the linewidth. The region between the plates is illuminated with resonance radiation from a Varian X49-609 spectral lamp filled with ^{133}Cs. The light is filtered so that only the D_1 line ($6\ ^2P_{1/2} \rightarrow 6\ ^2S_{1/2}$) is seen by the beam atoms. In the lamp line, the hfs of the $6\ ^2P_{1/2}$ state is not completely resolved and the lamp line consists of a doublet, the components of which are separated by the hfs of the ground state. With this apparatus, the precision is limited by the width of the lamp line, about 1500 MHz (50 mK). However, the precision may be substantially improved by passing the filtered light through an optically dense ^{133}Cs absorption beam. As shown in Fig. 4, the absorption cell consists essentially of a source oven and a collimator kept at the temperature of liquid nitrogen so as to reduce the Doppler velocity of the absorption beam. The effect of the absorption beam is to remove a doublet from each of the lamp lines. The two components of the doublet are separated by the hfs of the $6\ ^2P_{1/2}$ state of ^{133}Cs. In our experiment the width of the absorption lines varies from 150 to 250 MHz (3 to 8 mK). In principle, this width can be made as low as the natural linewidth, which for the cesium resonance line is about 10 MHz. However, such high precision would demand an electric field that is homogeneous and reproducible to better than 0.5×10^{-3} at field of almost 0.5×10^6 V/cm; this is presently beyond our capability.

The narrow gap between the electric field plates is used as a state selector so that we can at will refocus atoms either with $m_J(A) = 1/2$ or with $m_J(A) = -1/2$. For cesium isotopes with large nuclear spin and hence with the two hyperfine states, $F = I + 1/2$ and $F = I - 1/2$, about equally populated, this is essentially equivalent to refocusing atoms in

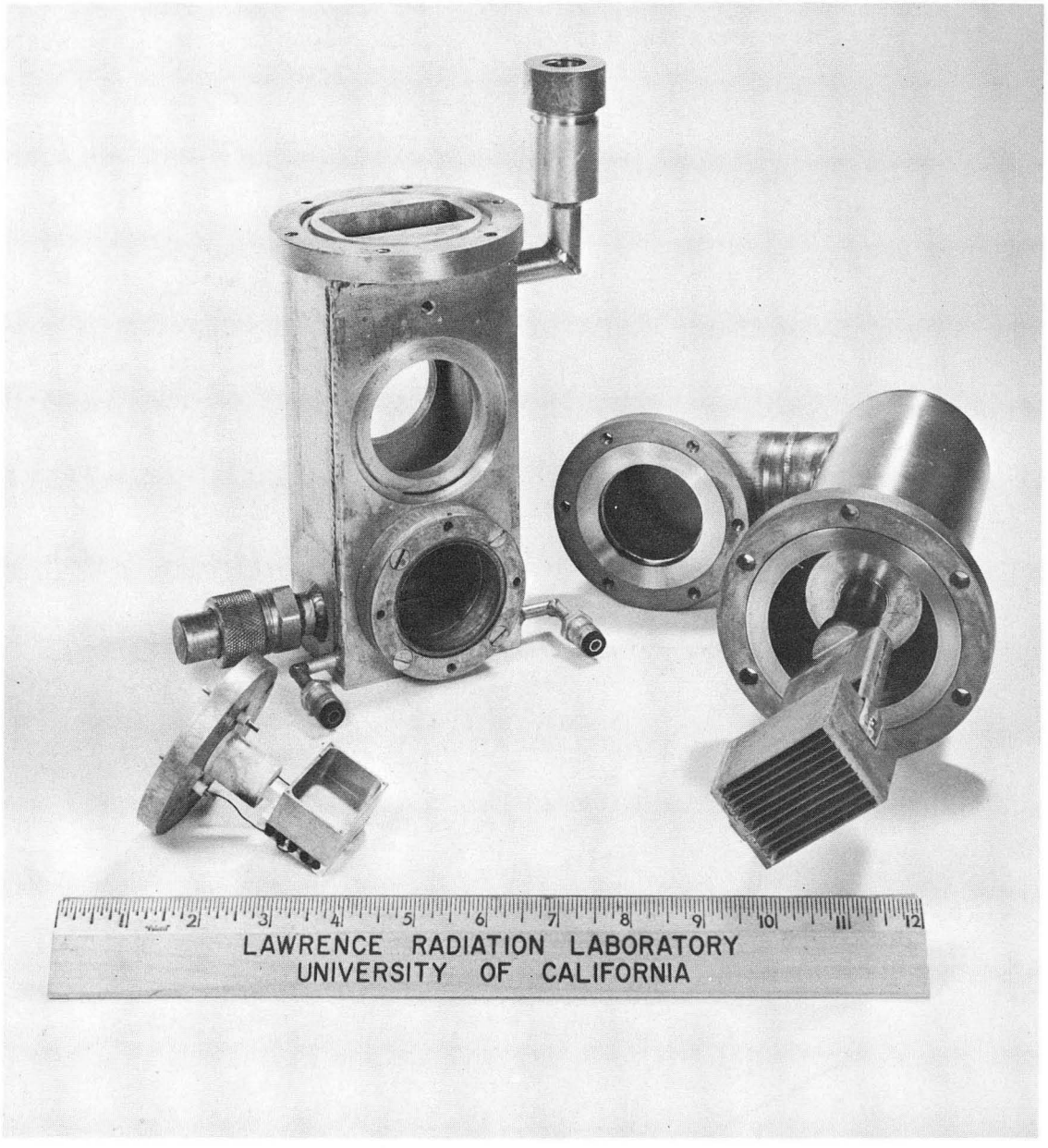

XBB 685-3072

Fig. 4. Absorption cell assembly.

either of the two hyperfine states. However, for ^{127}Cs and ^{129}Cs which have I = 1/2 all the atoms with $m_J(A) = 1/2$ belong to the F = 1 state while atoms with $m_J(A) = -1/2$ are equally distributed between the two states, F = 1 and F = 0; therefore refocusing a m_J state is not equivalent to refocusing the hyperfine states.

The Cs atomic beam is produced by heating the sample, in the form of a chloride or iodide, with calcium metal chips in the oven (see Fig. 5); calcium reduces cesium halides at temperatures of about 400° C, giving out cesium metal.

Stable cesium can be detected with a rhenium hot wire. Since the ionization potential of cesium is less than the work function of rhenium, Cs atoms that hit the wire are boiled off as ions and accelerated to a collector plate where the resulting current is measured with an electrometer. The detector for the radioactive isotopes are freshly flamed platinum foils which are shown in Fig. 6 together with the holders. The atoms that are refocused strike and stick to the platinum foil. After exposure the foils are taken out of the beam machine and counted in a continuous flow methane beta counter, shown in Fig. 7.

C. Stark Tuning

1. Without Absorption Beam

Consider the action of a ^{133}Cs atom in the atomic beam irradiated by the resonance radiation. At zero electric field the absorption lines of atoms in the beam coincide with the center of the emission lines in the lamp. Consequently, resonance absorption of photons takes place. In the subsequent decay, half of the atoms will undergo spin-flip and will contribute to the flop-in signal at the detector. As the electric

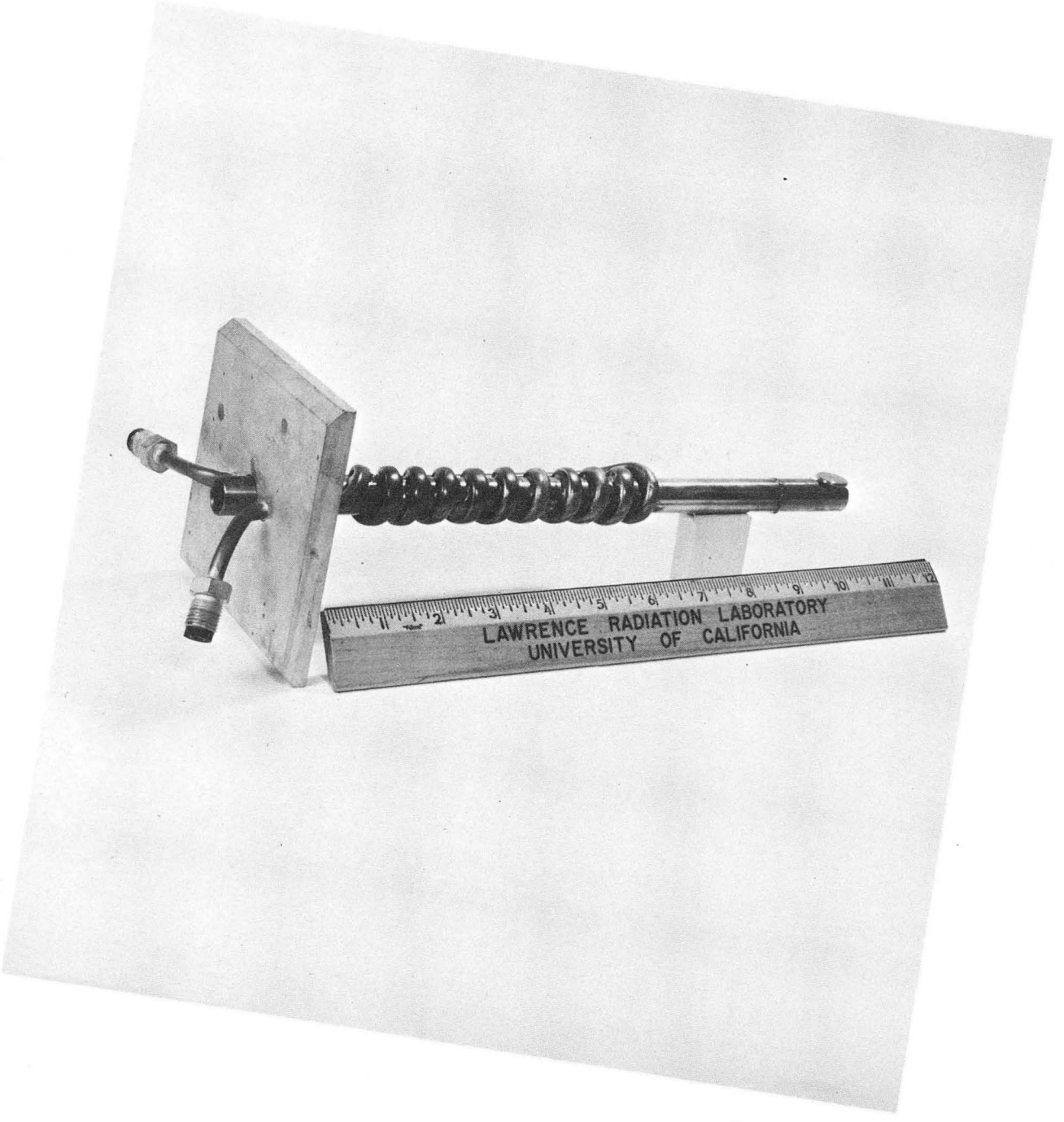

XBB 685-3073

Fig. 5. Oven and its loader.

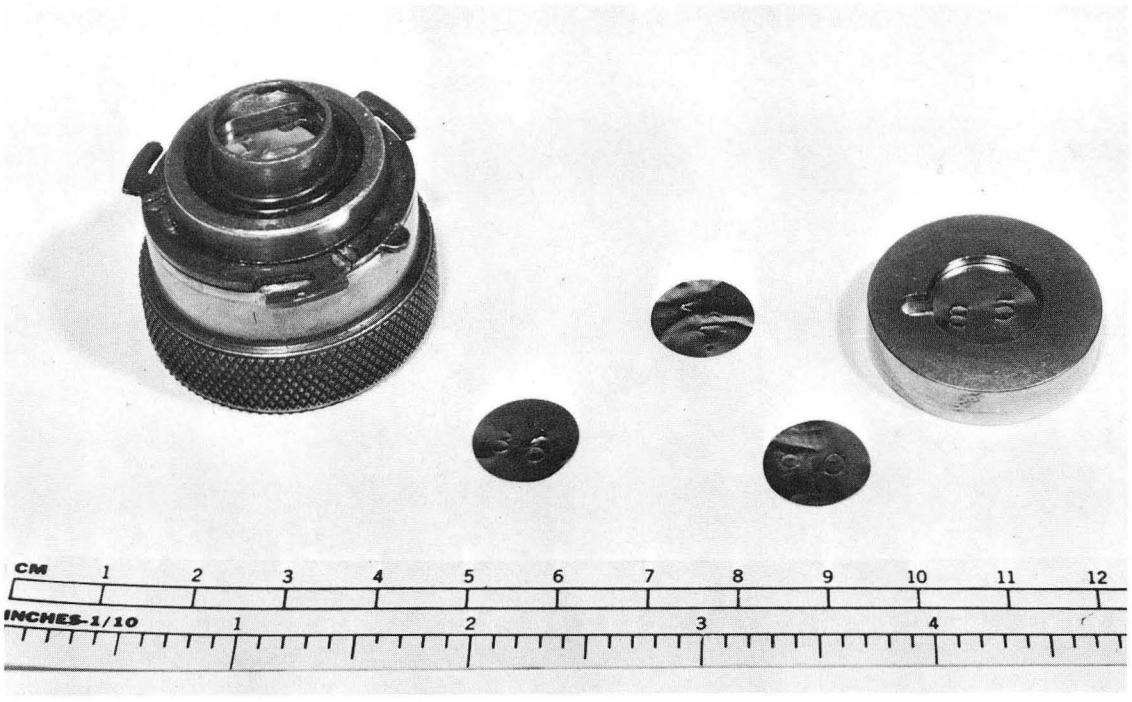

XBB 6711-6664

Fig. 6. Platinum foils (0.001 in. thick) shown with beam machine button holder and beta counter holder.

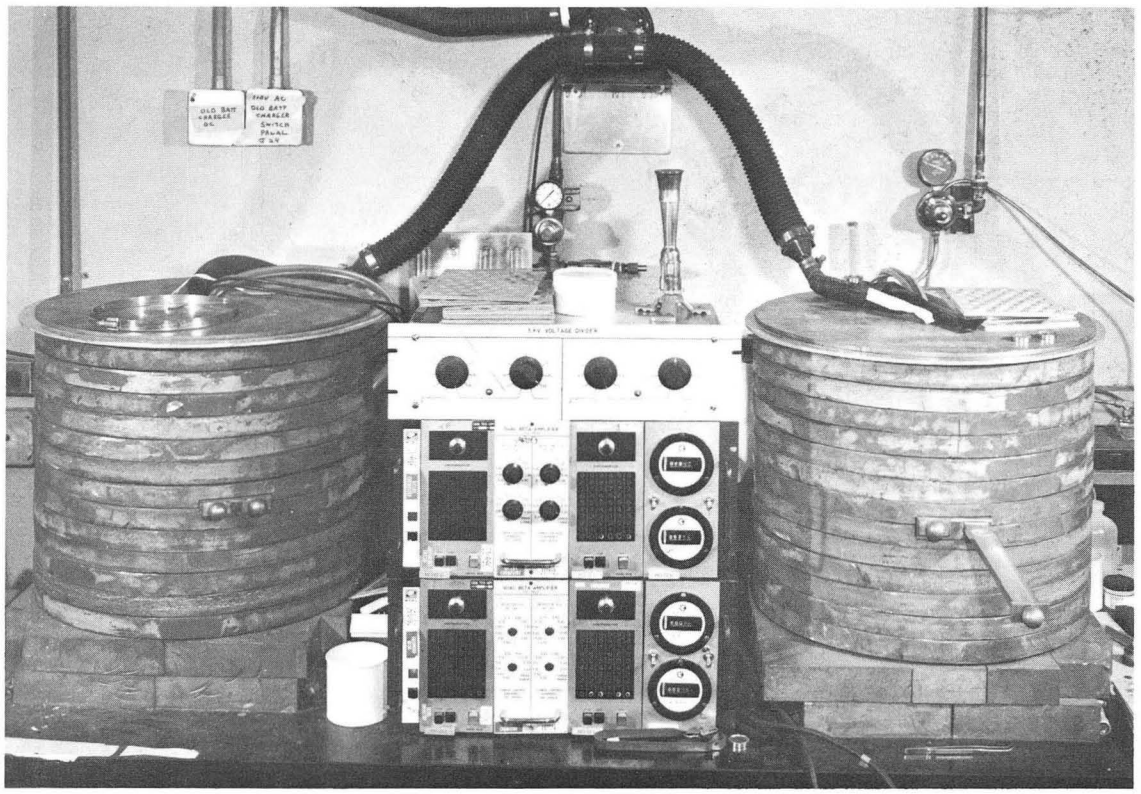

XBB 6711-6662

g. 7. Beta counters and associated electronics.

field is turned on, the Stark effect shifts the center of the absorption lines to lower frequencies until resonant absorption no longer occurs and the flop-in signal goes to zero. However, when the electric field is sufficiently large so as to shift the absorption lines by an amount equal to the ground-state hyperfine structure, a new overlap of the absorption lines with the emission lines of the lamp occurs, and another flop-in signal is observed (see Fig. 8a). In this way the Stark shift can be measured in the D_1 line; and from the V^2 dependence characteristic of the Stark effect a calibration of frequency shift versus applied voltage squared is obtained.

If the atomic beam consists of atoms of some other cesium isotope, then because of the different ground-state hyperfine structure, the different nuclear spin and the isotope shift, there is in general no signal at zero electric field. However, if the frequency of the absorption lines is displaced to the high-frequency side of either of the emission lines of the lamp, then the application of a suitable voltage brings the absorption lines into coincidence with the emission lines and a signal is observed at the detector. In Figs. 9 and 10 are shown the observed signals for a ^{134}Cs and a ^{137}Cs beam, respectively.

2. With Absorption Beam

As mentioned above, the effect of the absorption beam is to remove a doublet from each of the lamp lines; the two components of the doublet are separated by the hfs of the $6\ ^2P_{1/2}$ of ^{133}Cs. The observed ^{133}Cs intensity pattern in this case is shown in Fig. 8b and can be understood with reference to the energy-level diagrams shown in Fig. 11. At zero electric field the absorption lines of the ^{133}Cs atomic beam overlap the

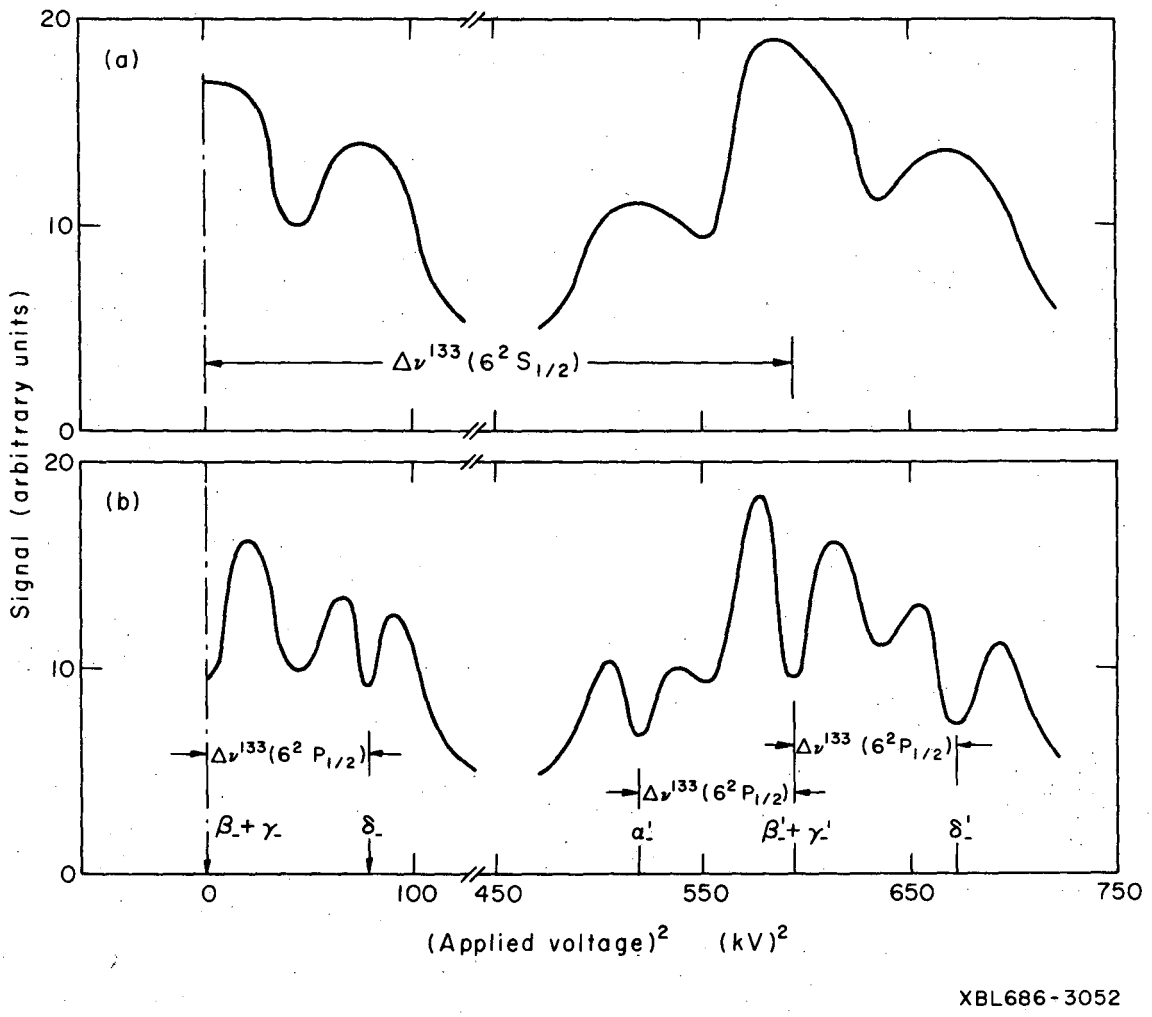

Fig. 8. Observed ^{133}Cs signal versus square of applied voltage; (a) without absorption beam, (b) with absorption beam.

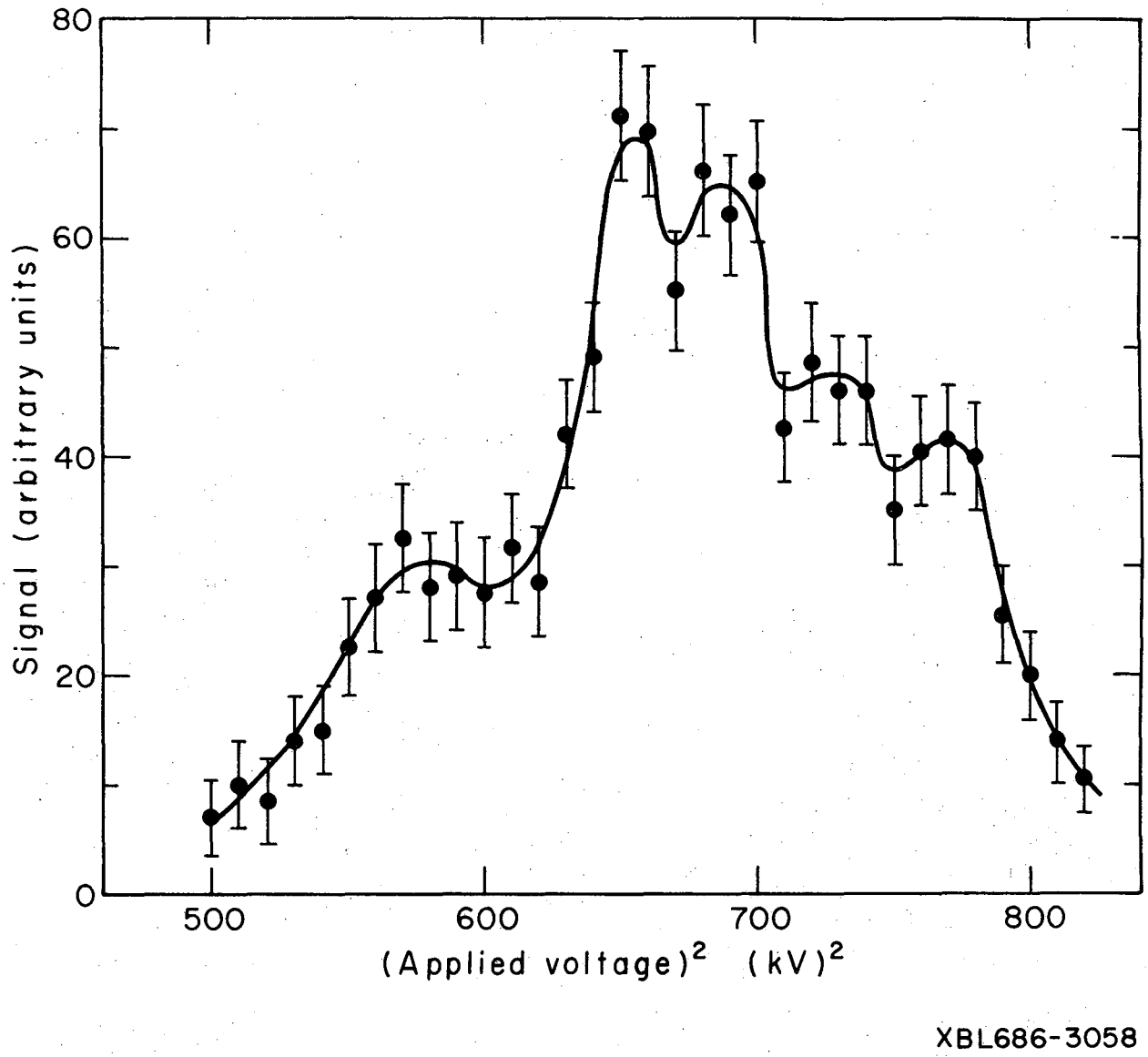

Fig. 9. Observed signal versus square of applied voltage for a ^{134}Cs beam.

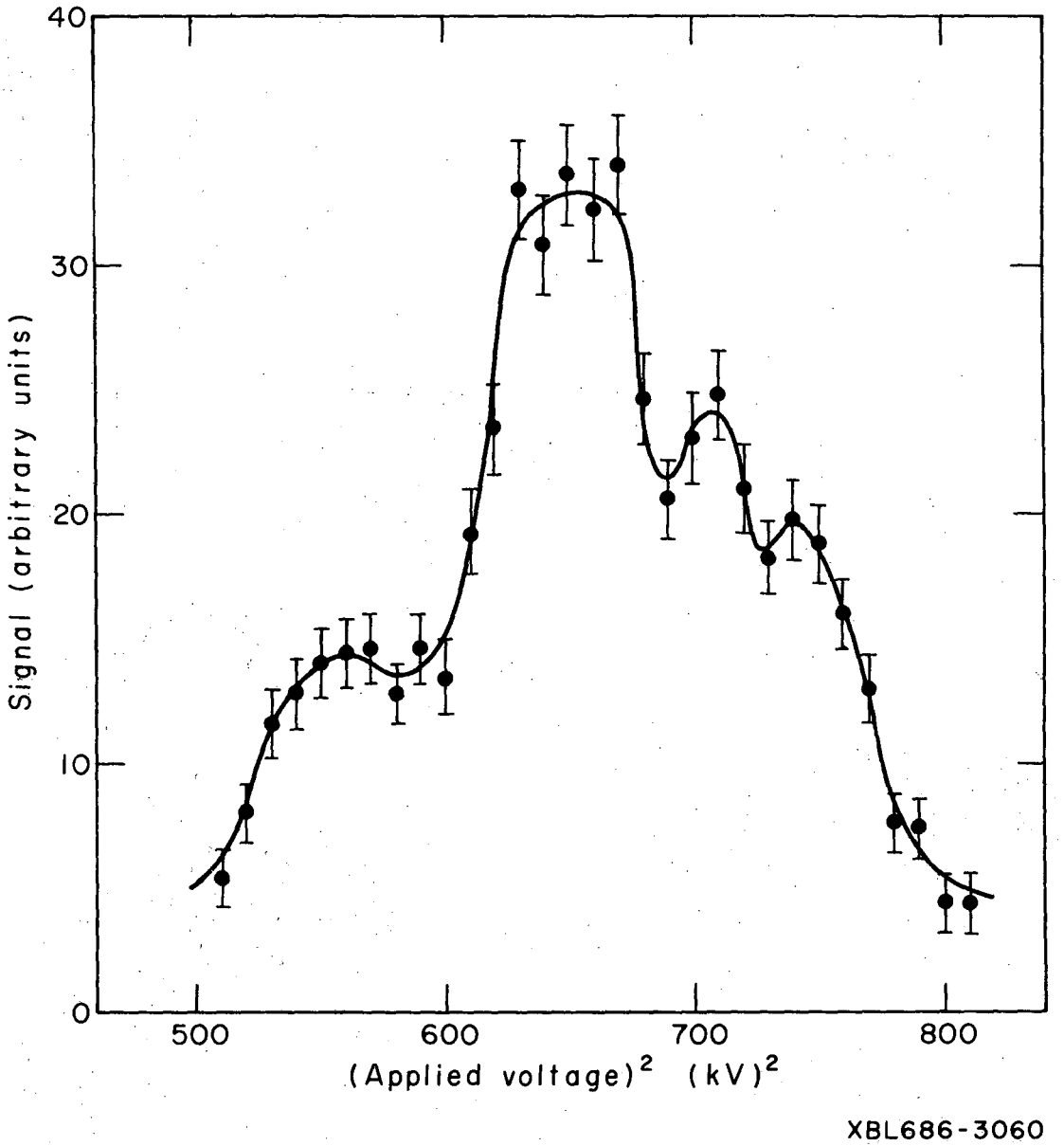

Fig. 10. Observed signal versus square of applied voltage for a ^{137}Cs beam.

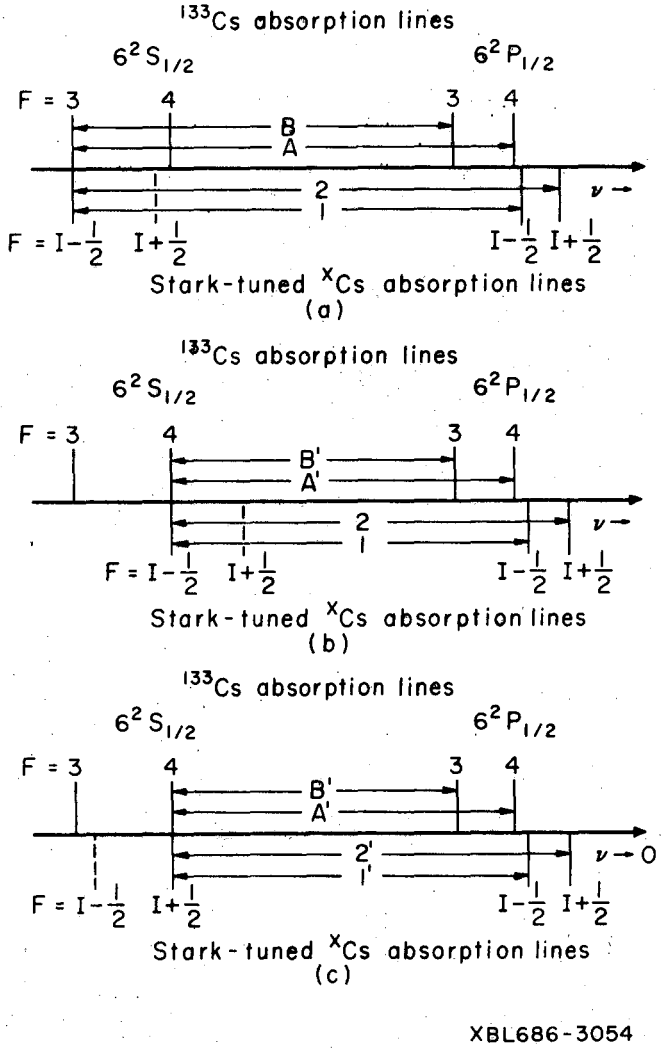

Fig. 11. Labeling of the intensity minima. (a) α_-: coincidence of beam-absorption line 1 with ^{133}Cs absorption line A; β_-: coincidence of 2 with A; σ_-: coincidence of 1 with B; δ_-: coincidence of 2 with B. (b) α'_-: coincidence of 1 with A'; β'_-: coincidence of 2 with A'; σ'_-: coincidence of 1 with B'; δ'_-: coincidence of 2 with B'. (c) α_+: coincidence of 1' with A'; β_+: coincidence of 2' with A'; σ_+: coincidence of 1' with B'; δ_+: coincidence of 2' with B'.

absorption lines of the ^{133}Cs absorption beam, and a minimum in the intensity curve is observed. However, as the electric field is turned on, the Stark effect decreases the frequency of the absorption lines of the atoms in the beam apparatus, and the observed signal increases. However, when the electric field is sufficient to shift the frequency by an amount equal to the hfs of the excited ($6\ ^2P_{1/2}$) state, a second intensity minimum is observed. At higher electric fields when the frequency is shifted by an amount equal to the ground-state hfs, the beam absorption line is brought into resonance with the second lamp-emission line. Here three intensity minima are observed. These three minima are equally spaced and correspond to a shift by an amount equal to the hfs of the $6\ ^2P_{1/2}$ state.

As can be seen from the energy-level diagram, the separation between the two minima labeled $\beta_- + \gamma_-$ and $\beta'_- + \gamma'_-$, in Fig. 8b, corresponds to a Stark shift of the energy levels equal to 9192 MHz, the approximate hfs of the ^{133}Cs ground state. Using this as a calibration and taking the separations between $\beta_- + \gamma_-$ and δ_-, between α'_- and $\beta'_- + \gamma'_-$, and between $\beta'_- + \gamma'_-$ and δ'_-, as equal to the hfs of the $6\ ^2P_{1/2}$ state of ^{133}Cs, we obtain[19]

$$\Delta\nu^{133}\ (6\ ^2P_{1/2}) = 1167 \pm 40\ \text{MHz} \quad .$$

This value is in good agreement with the value (1173 ±10 MHz) obtained by conventional optical spectroscopy.[20]

A similar situation pertains when the atomic beam consists of some other cesium isotope, ^{X}Cs. Whenever the Stark tuning brings about an overlap of the beam-absorption lines with the lamp-emission lines, there are, however, as can be seen from Fig. 11, four possible overlap positions of the Stark-shifted energy levels of ^{X}Cs beam atoms with the unshifted

levels of ^{133}Cs atoms in the absorption cell. These overlap positions correspond to minima in the observed intensity pattern. From Fig. 11 it is also apparent that the separation between the minima α and γ and between β and δ corresponds to the hfs of the 6 $^2P_{1/2}$ state of ^{X}Cs, while the separation between α and β and between γ and δ corresponds to the hfs of the 6 $^2P_{1/2}$ state of ^{133}Cs. Thus from the position of the intensity minima we can obtain the hfs of the 6 $^2P_{1/2}$ state of ^{X}Cs, and further, with a knowledge of the ground-state hyperfine structure (see Table I), infer the ^{X}Cs - ^{133}Cs isotope shift.

Table I. Some Relevant Quantities of the Cesium Isotopes.*

Cesium Isotope	Half-life $\tau_{1/2}$	Nuclear Spin I	μ_I in n.m.	$\Delta\nu(6\ ^2S_{1/2})$ in MHz
127	6.2 h	1/2	1.44(3)	8900(150)
129	31 h	1/2	1.48(3)	9229(30)
133		7/2	2.574(13)	9192.63177
134	2.2 y	4	2.9901(12)	10469(12)
134m	2.9 h	8	1.0964(9)	3684.5(5)
137	30 y	7/2	2.8379(9)	10115.527(15)

* All taken from Ref. 21 except the values for the nuclear magnetic moment of ^{127}Cs and ^{129}Cs that are taken from Ref. 22.

V. EXPERIMENTAL RESULTS

A. Sample Preperation

1. The Isotopes ^{127}Cs and ^{129}Cs

The isotopes ^{127}Cs and ^{129}Cs are made through the reactions ^{127}I (α, 4n) ^{127}Cs and ^{127}I (α, 2n) ^{129}Cs respectively, by bombarding ^{127}I in the 88-inch Cyclotron at Berkeley with α-particles of the appropriate energies. For the production of ^{127}Cs the energy of the bombarding α-particles is 70 Mev, and for the production of ^{129}Cs it is 45 Mev. In Fig. 12 is shown the cyclotron target.

The desired radioactive isotope (^{127}Cs or ^{129}Cs) is produced in the form of an iodide. In order to extract this from the bombarded target, the following chemical procedure is followed. The bombarded iodine target is boiled in a beaker with carbon tetrachloride, a good iodine solvent, and water to which has been added a suitable amount of the stable carrier to serve the purposes of field calibration and beam normalization. With a lower boiling temperature and smaller latent heat of vaporization than water, the carbon tetrachloride is quickly boiled away, together with almost all of the iodine by sublimation. Boiling the remaining solution to dryness leaves the radioactive cesium with the stable carrier in the form of halides on the walls of the beaker. The beaker is then washed with water to dissolve the cesium halides, and the activity is transferred to a test tube. The solution is boiled down to about one cc. This condensed solution is then finally transferred into the oven and slowly heated to dryness.

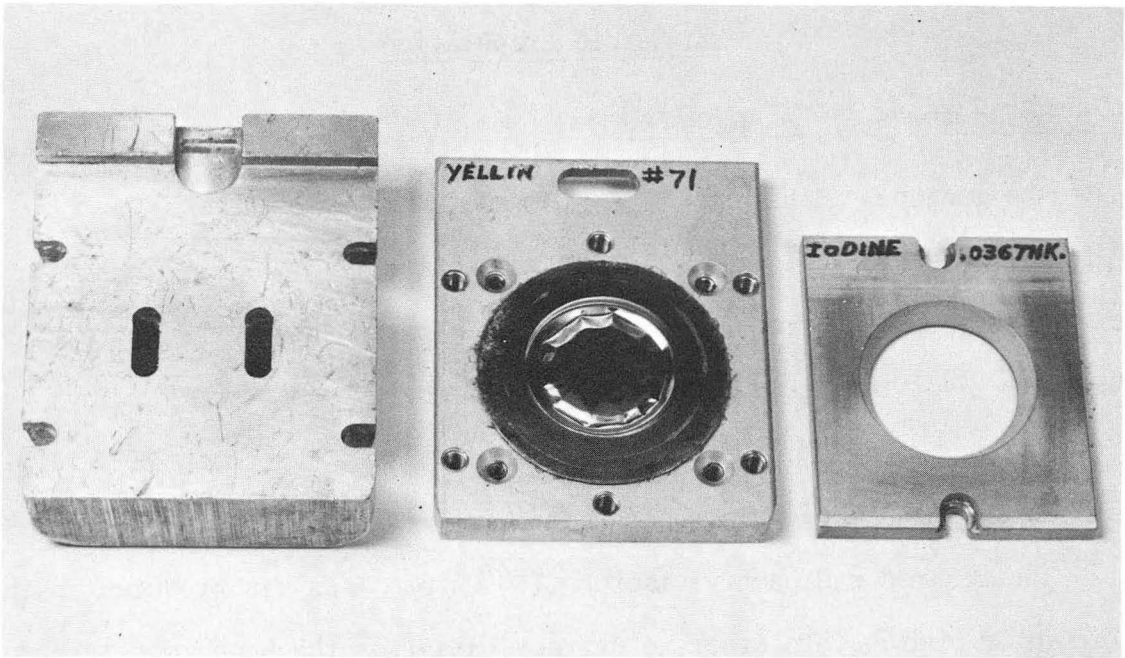

XBB 686-3991

Fig. 12. Water-cooled cesium target assembly.

2. The Isotopes ^{134}Cs and ^{134m}Cs

These two isotopes are made by the irradiation of the stable cesium (in the form of a chloride) in a nuclear reactor at the Lawrence Radiation Laboratory at Livermore at a flux of about 10^{13} neutrons cm^{-2}-sec^{-1} for either six hours (to produce ^{134m}Cs) or a week (to produce ^{134}Cs). In the former case the long-lived ^{134}Cs (2.2 y) is produced only in a negligible amount; in the latter case the quantity of ^{134m}Cs is, because of its much smaller half-life (2.9 h), sufficiently reduced a couple of weeks after the shutdown so as not to interfere experimentally.

3. The Isotope ^{137}Cs

The isotope ^{137}Cs can be purchased from the Oak Ridge National Laboratory as a fission product. It comes in the form of a chloride. In order to get a homogeneous mixture, the sample is dissolved in water with a suitable amount of stable cesium chloride. The solution is filtered to get rid of any appreciable quantity of the daughter (Ba) isotope, and boiled down in a test tube to a few droplets. The concentrated solution is then transferred into the oven and slowly heated to dryness.

B. Experimental Results

1. Hyperfine Structure of the $6\ ^2P_{1/2}$ State

It can be shown from Eqs. (68) and (73) that

$$\frac{\Delta\nu(6\ ^2S_{1/2})}{\Delta\nu(6\ ^2P_{1/2})} = -\frac{16\pi}{3}\ \mu_o|\psi(o)|^2\ \frac{J}{\langle B_z(o)\rangle_{JJ}}\ , \tag{84}$$

which is the same for all the cesium isotopes. Since all but ^{134m}Cs of the radioactive cesium isotopes concerned in this experiment have a ground-state hyperfine structure separation comparable to that of the

stable isotope, we should from Eq. (84) expect for these isotopes a value of the excited ($6\ ^2P_{1/2}$) state hyperfine structure separation comparable to 1173 MHz, the hyperfine structure of the $6\ ^2P_{1/2}$ state of ^{133}Cs. Consequently, the two minima β and γ, each having a width of 150-250 MHz, are not resolved. This is experimentally seen to be the case. In these cases the value of $\Delta\nu^X(6\ ^2P_{1/2})$ is determined from the separation between the minima α and δ, which is equal to $\Delta\nu^X(6\ ^2P_{1/2})$ plus $\Delta\nu^{133}(6\ ^2P_{1/2})$.

In principle, the hfs of the $6\ ^2P_{1/2}$ state of a radioactive isotope can be determined from the position of the intensity minima obtained in any of the three cases shown in Fig. 11. For ^{127}Cs and ^{129}Cs, both having a nuclear spin equal to 1/2, the minima α_-'s and β_-'s however do not exist. This is easily seen to be a consequence of the fact that the transition $F = 0\ (6\ ^2P_{1/2}) \rightarrow F = 0\ (6\ ^2S_{1/2})$ is forbidden, i.e. that the beam absorption line marked 1 is missing in Fig. 11a and Fig. 11b. Therefore, the hfs of the $6\ ^2P_{1/2}$ state of ^{127}Cs and ^{129}Cs can only be obtained from the overlapping configuration shown in Fig. 11c. Although the beam atoms with $m_J(A) = -1/2$ are initially equally distributed between the two hyperfine states $F = 1$ and $F = 0$ of the ground state of ^{127}Cs or ^{129}Cs, when these atoms are refocused there may be, however, a partial overlap of the minimum δ_+ with the minimum δ_-, arising from the comparable magnitude of the ground-state hfs of these two isotopes with that of ^{133}Cs. This partial overlap of the minima will broaden the width of the observed intensity minimum and add to the experimental error. Thus the minima α_+ and δ_+ are best located when the beam atoms with

$m_J(A) = 1/2$ are refocused. In this latter case, $\Delta\nu^{133}(6\ ^2P_{1/2}) = 1173$ MHz is used as a calibration.

For ^{134m}Cs, intensity minima arising from both the cases b and c of Fig. 11 are observed. For ^{134}Cs and ^{137}Cs only the case b gives a complete pattern; δ_- and δ_+ are also observable. In fact, the hfs of the $6\ ^2P_{1/2}$ state of ^{137}Cs is determined from the separation between the minima δ_- and α'_-, which is equal to $\Delta\nu^{133}(6\ ^2S_{1/2}) - \Delta\nu^{133}(6\ ^2P_{1/2}) - \Delta\nu^{137}(6\ ^2P_{1/2})$. The minimum δ'_- for ^{137}Cs is skipped just because of an arcing problem of the field-plates at high fields.

Some typical observed intensity patterns are shown in Figs. 13-17 for the radioactive cesium isotopes. The final results, as obtained from the data tabulated in Tables II-VI, are

$$^{127}(6\ ^2P_{1/2}) = 1160 \pm 45 \text{ MHz}$$

$$^{129}(6\ ^2P_{1/2}) = 1243 \pm 45 \text{ MHz}$$

$$^{134m}(6\ ^2P_{1/2}) = 541 \pm 36 \text{ MHz}$$

$$^{134}(6\ ^2P_{1/2}) = 1324 \pm 30 \text{ MHz}$$

$$^{137}(6\ ^2P_{1/2}) = 1275 \pm 45 \text{ MHz} \quad .$$

The values are in good agreement with those as follows obtained from Eq. (84) by using the known values for the ground-state hfs of the isotopes and taking the value for the $6\ ^2P_{1/2}$ state hfs of ^{133}Cs to be 1173 MHz:

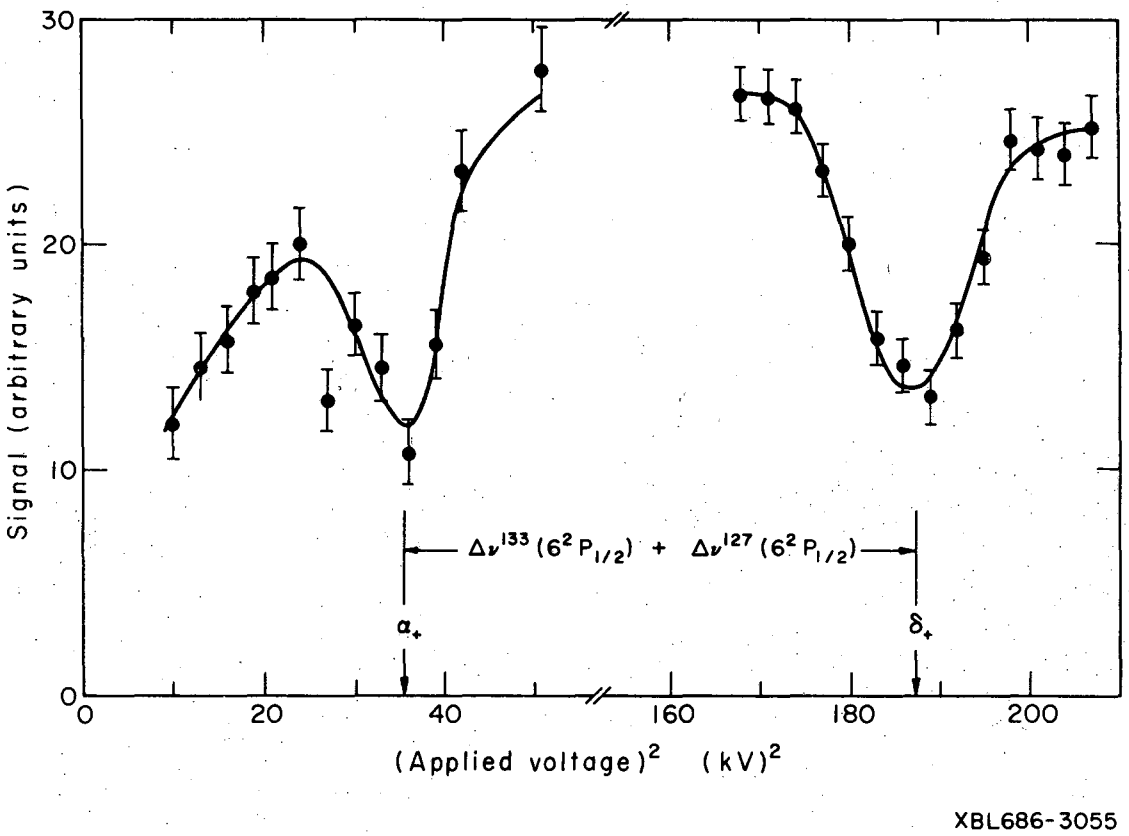

Fig. 13. Observed ^{127}Cs signal versus square of applied voltage.

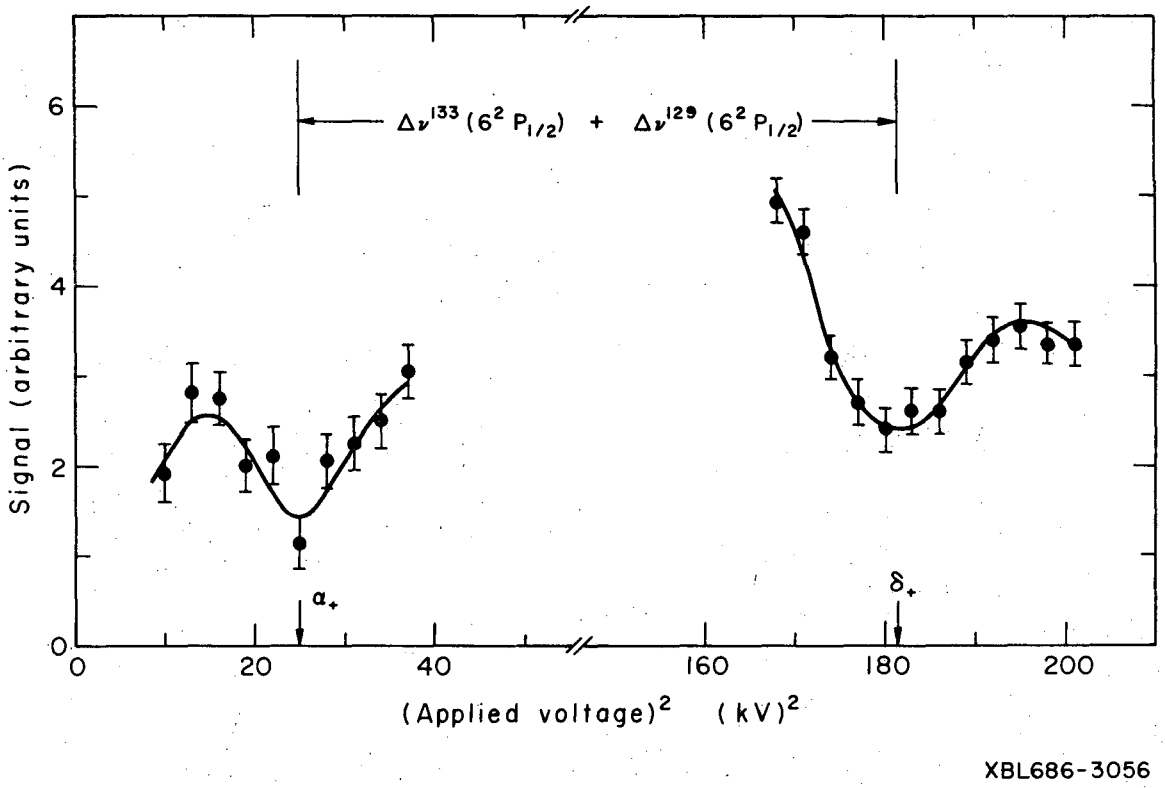

Fig. 14. Observed ^{129}Cs signal versus square of applied voltage.

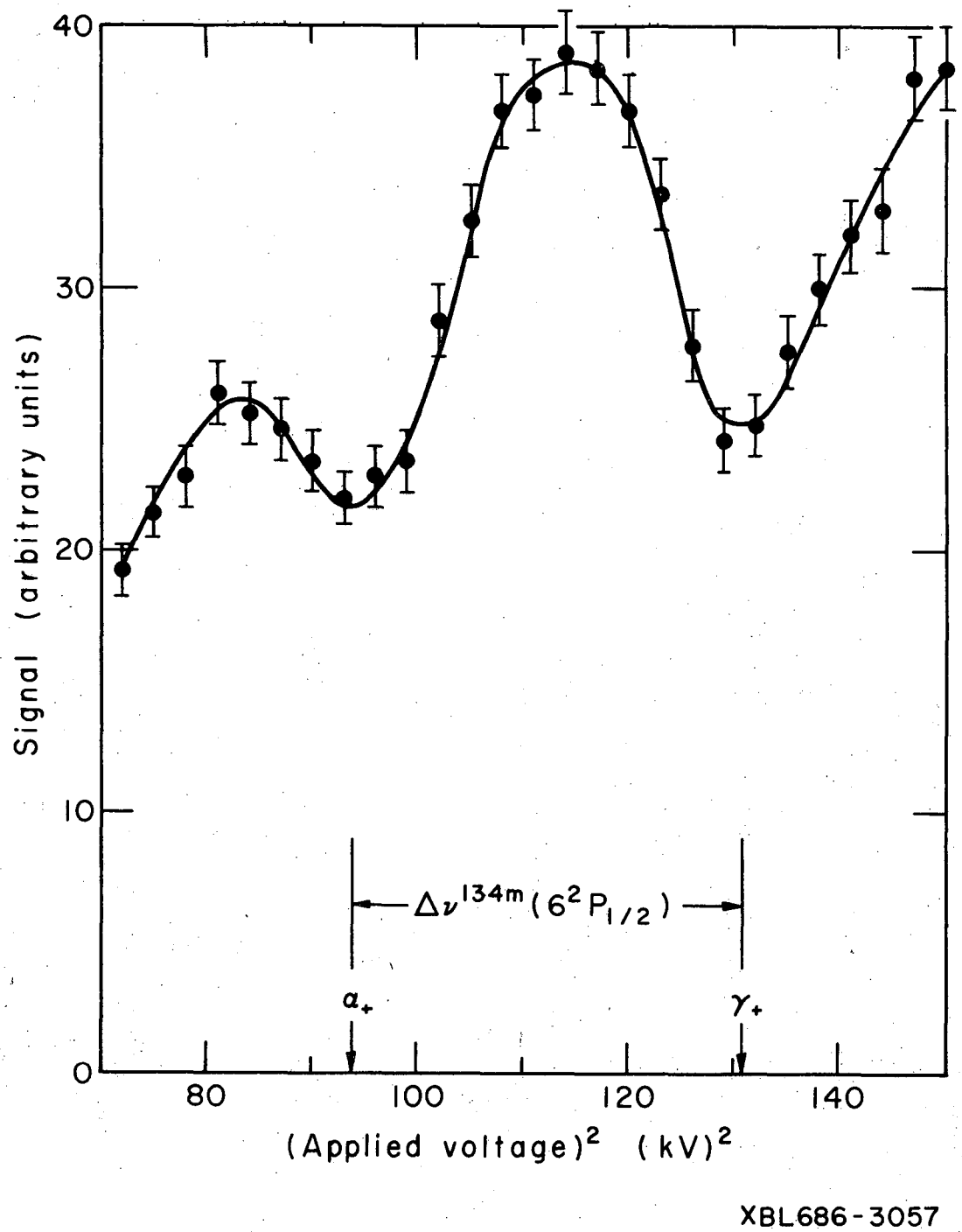

Fig. 15. Observed ^{134m}Cs signal versus square of applied voltage.

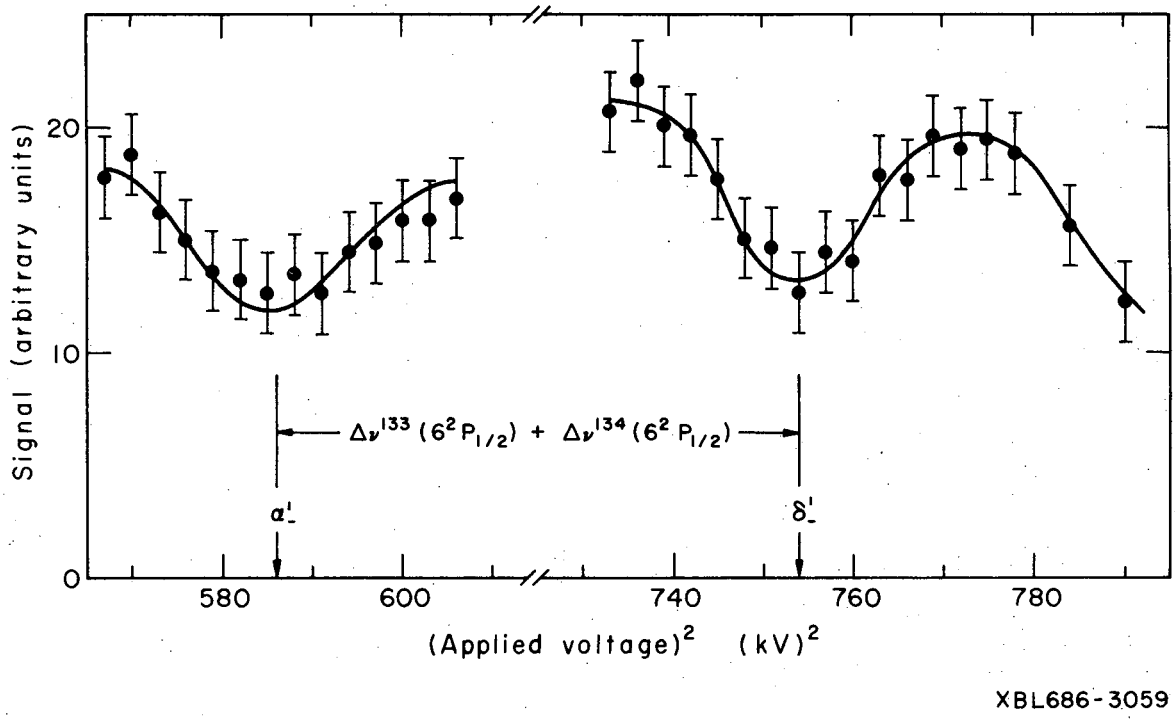

Fig. 16. Observed ^{134}Cs signal versus square of applied voltage.

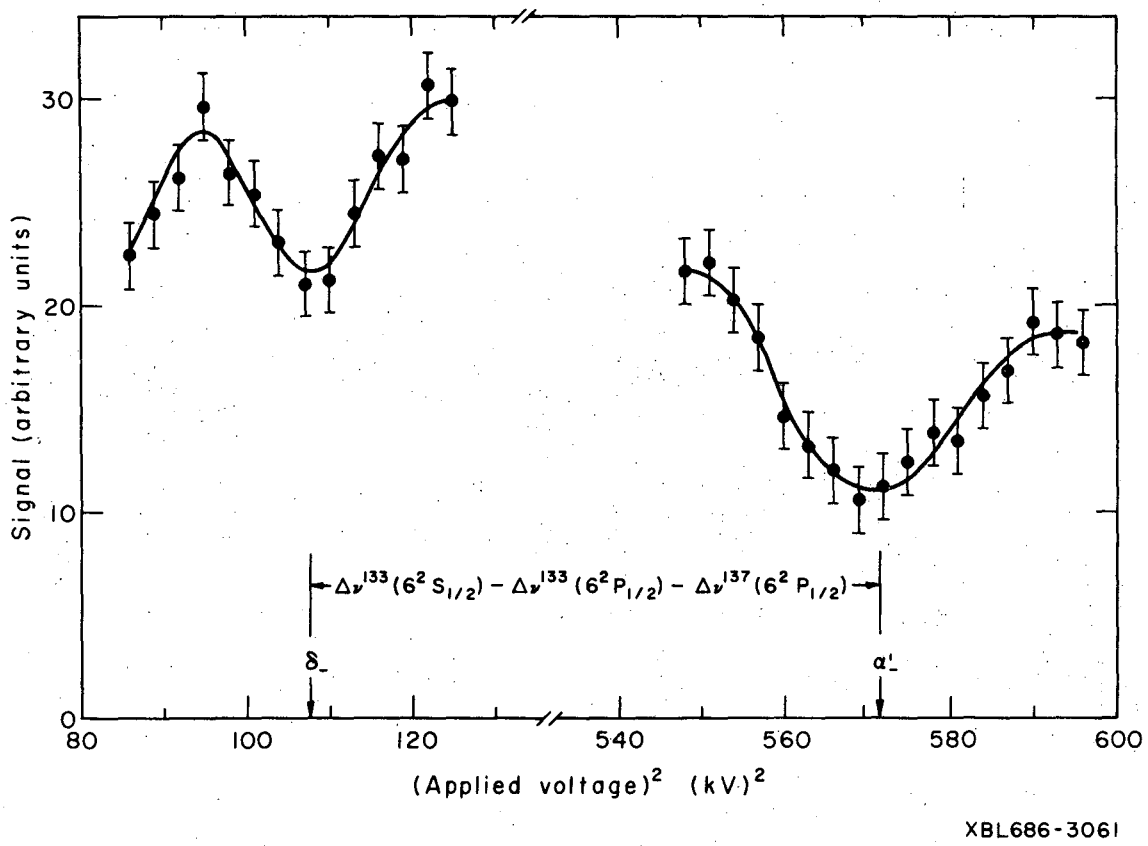

Fig. 17. Observed ^{137}Cs signal versus square of applied voltage.

Table II. ^{127}Cs Stark Shift Data

Intensity Minimum	Calibration MHz/(kV)^2	Stark Shift (kV)^2	Stark Shift MHz
α_+	15.64 ±0.05	34.0 ±1.5	532 ±25
α_+	15.12 ±0.05	36.0 ±1.5	544 ±25
δ_+	15.36 ±0.05	187.0 ±2.5	2872 ±48
α_+	14.48 ±0.05	37.0 ±2.0	543 ±31

Table III. ^{129}Cs Stark Shift Data

Intensity Mimimum	Calibration MHz/(kV)^2	Stark Shift (kV)^2	Stark Shift MHz
α_+	15.17 ±0.05	25.0 ±2.0	379 ±32
δ_+	15.64 ±0.05	181.0 ±2.5	2831 ±48
α_+	15.48 ±0.05	29.0 ±2.0	449 ±32

Table IV. ^{134m}Cs Stark Shift Data

Intensity Minimum	Calibration MHz/(kV)^2	Stark Shift (kV)^2	Stark Shift MHz
α'_-	15.40 ±0.05	332.0 ±2.0	5113 ±47
β'_-	15.40 ±0.05	411.0 ±2.0	6329 ±51
σ'_-	15.40 ±0.05	365.0 ±2.0	5621 ±49
δ'_-	15.40 ±0.05	443.0 ±2.0	6822 ±53
α_+	15.70 ±0.05	93.0 ±1.5	1460 ±28
α_+	15.64 ±0.05	94.0 ±2.0	1470 ±36
σ_+	15.64 ±0.05	128.0 ±4.0	2002 ±69
α_+	15.36 ±0.05	93.5 ±2.0	1436 ±35
σ_+	15.36 ±0.05	130.0 ±4.0	1997 ±68
α_+	15.56 ±0.05	90.0 ±3.0	1440 ±51
α_+	15.36 ±0.05	94.0 ±3.0	1444 ±51
σ_+	15.36 ±0.05	131.0 ±3.0	2012 ±53

Table V. ^{134}Cs Stark Shift Data

Intensity Minimum	Calibration MHz/(kV)^2	Stark Shift (kV)^2	Stark Shift MHz
δ_+	14.48 ±0.04	44.0 ±4.0	637 ±60
δ_+	14.39 ±0.04	47.0 ±2.0	676 ±31
δ_+	14.48 ±0.04	45.0 ±1.5	652 ±24
δ_-	14.30 ±0.04	136.0 ±3.0	1945 ±48
δ_-	14.48 ±0.04	135.0 ±2.0	1955 ±34
α'_-	14.76 ±0.01	585.0 ±3.0	8635 ±50
δ'_-	14.73 ±0.01	757.0 ±3.0	11151 ±52
α'_-	14.76 ±0.01	587.0 ±2.0	8664 ±35
δ'_-	14.73 ±0.01	757.0 ±3.0	11151 ±52

Table VI. ^{137}Cs Stark Shift Data

Intensity Minimum	Calibration MHz/(kV)^2	Stark Shift (kV)^2	Stark Shift MHz
δ_-	14.39 ±0.03	109.0 ±3.0	1569 ±46
α'_-	14.42 ±0.03	575.0 ±3.0	8292 ±52
α'_-	14.45 ±0.04	574.0 ±3.0	8294 ±65
δ_-	14.48 ±0.03	102.0 ±3.0	1549 ±46
δ_-	14.48 ±0.03	108.0 ±2.0	1564 ±32
α'_-	14.59 ±0.04	570.0 ±4.0	8316 ±80
α'_-	14.54 ±0.04	572.0 ±3.0	83.7 ±66

$$^{127}(6\ ^2P_{1/2})(\text{calc}) = 1136\ \text{MHz}$$

$$^{129}(6\ ^2P_{1/2})(\text{calc}) = 1178\ \text{MHz}$$

$$^{134m}(6\ ^2P_{1/2})(\text{calc}) = 470\ \text{MHz}$$

$$^{134}(6\ ^2P_{1/2})(\text{calc}) = 1336\ \text{MHz}$$

$$^{137}(6\ ^2P_{1/2})(\text{calc}) = 1291\ \text{MHz}\ .$$

2. Isotope Shift in the D_1 Line

From the measured hyperfine structure of the $6\ ^2P_{1/2}$ state and the position of any of the intensity minima, the isotope shift relative to ^{133}Cs of a radioactive cesium isotope can easily be determined as follows. With reference to Fig. 18, it is evident that

$$IS(^{127}Cs - ^{133}Cs) = \left[\frac{1}{4}\Delta\nu^{127}(6\ ^2S_{1/2})+\delta_+ - \frac{1}{4}\Delta\nu^{127}(6\ ^2P_{1/2})\right] - \left[\frac{7}{16}\Delta\nu^{133}(6\ ^2S_{1/2})+\frac{9}{16}\Delta\nu^{133}(6\ ^2P_{1/2})\right]$$

$$= +\ 177\ \pm 45\ \text{MHz}$$

$$= +\ 5.9(1.5) \times 10^{-3}\ \text{cm}^{-1}\ .$$

Similarly, we obtain

$$IS(^{129}Cs - ^{133}Cs) = +2.8(1.5) \times 10^{-3}\ \text{cm}^{-1}$$

$$IS(^{133}Cs - ^{134m}Cs) = -2.2(1.2) \times 10^{-3}\ \text{cm}^{-1}$$

$$IS(^{133}Cs - ^{134}Cs) = +1.8(1.0) \times 10^{-3}\ \text{cm}^{-1}$$

$$IS(^{133}Cs - ^{137}Cs) = -6.0(1.5) \times 10^{-3}\ \text{cm}^{-1}\ .$$

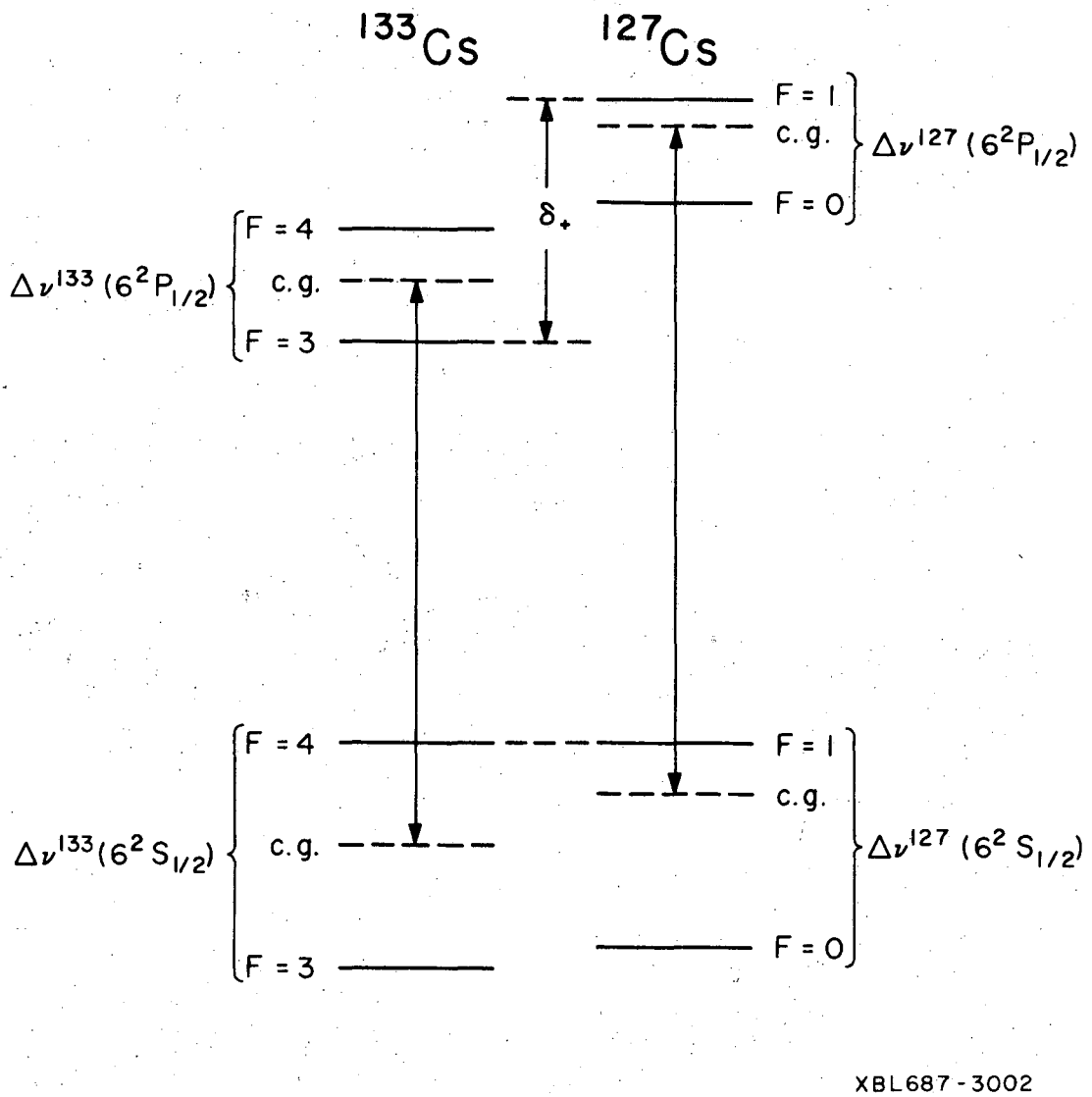

Fig. 18. Schematic energy level diagram for the determination of the ^{127}Cs - ^{133}Cs isotope shift.

Here a positive sign means that the wave number of the D_1 line for the indicated isotope is greater than that for ^{133}Cs.

C. Calculation of Nuclear Deformation from the Isotope Shift

The total observed isotope shift is a sum of the contributions from the mass effects and the field effect, i.e.

$$\delta(\Delta E)_{total} = \delta(\Delta E)_{nor.\ mass} + \delta(\Delta E)_{sp.\ mass} + \delta(\Delta E)_{field} \qquad (85)$$

where it is now assumed that the values of $\delta(\Delta E)$ apply to the differences in the upper and lower levels involved in the D_1 transition. The normal mass shift can be calculated from Eq. (9) and is found to be -0.34×10^{-3} cm^{-1} for the isotope pair ^{133}Cs - ^{134}Cs. A recent recalculation by Bauche[23] shows that the specific mass shift, which is given to be $+0.38 \times 10^{-3}$ cm^{-1} for the same pair, almost cancels the normal mass shift. Under this favorable condition the mass shifts may entirely be neglected and Eq. (85) may be rewritten as

$$\delta(\Delta E)_{total} = \delta(\Delta E)_{field} \ . \qquad (86)$$

Fradkin[24] has given an estimate of the ratio of the isotope shifts arising from s and $p_{1/2}$ electrons of the same principle quantum number; this is equal to $a^2/(1+\sigma)^2$ (where a and σ are as defined in section 11B), assuming hydrogen-like Schroedinger wave function. Its numerical value for cesium is about 0.04. Huehnermann and Wagner[25] have obtained for the ^{133}Cs - ^{134}Cs isotope shift in the D_1 and D_2 lines the respective values of $+1.17(5) \times 10^{-3}$ cm^{-1} and $+1.25(6) \times 10^{-3}$ cm^{-1}. If we assume a cancellation of the mass effects in the D_2 line also, the difference between these two values can then be explained as the isotope shift of

the 6 $^2P_{1/2}$ state. This corresponds to a ratio of 0.06. Therefore, the assumption of no isotope shift for the $p_{1/2}$ electron seems to be well justified, if we are interested in only getting something of a qualitative nature out of the isotope shift data.

Under this assumption we may then write, using Eq. (52) and $\alpha^2 = \frac{5}{4\pi}\beta^2$,

$$\delta(\Delta E)_{total} = \Delta E_{sph}\left[2\sigma\frac{\delta R_o}{R_o} + \sigma\frac{5}{4\pi}\delta(\beta^2)\right] \tag{87}$$

where ΔE_{sph} is given by Eq. (23) and $R_o = 1.2A^{1/3} \times 10^{-13}$ cm. This relation permits us to calculate the squared nuclear deformation parameters of the isotopes from the isotope shift data. In Table VII are presented the results to date on the isotope shifts (measured with respect to ^{133}Cs) of eight cesium isotopes in the nuclear ground state. In the case of ^{131}Cs and ^{132}Cs, the isotope shifts are measured in the D_2 line. Assuming no isotope shift for the 6 $^2P_{1/2}$ state, they serve our purpose well; and no correction is made.

Table VII gives also the spectroscopic quadrupole moments and the intrinsic quadrupole moments obtained from the formula

$$Q_o = \frac{(I+1)(2I+3)}{I(2I-1)}Q \tag{88}$$

where Q_o is the intrinsic quadrupole moment and Q the spectroscopic quadrupole moment.

In the evaluation of ΔE_{sph}, the value of $|\psi(o)|^2$ used is the average of the values obtained with the aid of Eq. (73) from the known nuclear magnetic moments and ground-state hfs of the isotopes. These values are given in Table VIII, together with the A_s's. The normal volume effect is calculated to be 10.7×10^{-3} cm^{-1} per addition of one neutron.

Table VII. Isotope Shift and Nuclear Quadrupole Moments*

Cesium Isotope	IS in 10^{-3} cm^{-1} (relative to ^{133}Cs)	Q barns	Q_o barns
127	+5.9 ±1.5		
129	+2.8 ±1.5		
131	-0.33 ±0.05	-0.59 ±0.01	-1.596
132	+1.72 ±0.05	+0.46 ±0.01	+1.610
133	0	-0.003 ±0.002	-0.006
134	+1.8 ±(1.0)	+0.356 ±0.002	+0.699
135	-1.23 ±0.11	+0.049 ±0.002	+0.105
137	-6.0 ±1.5	+0.050 ±0.002	+0.107

* Values not obtained in this experiment are taken from Refs. 26-31.

Table VIII. Values of A_s and $|\psi(o)|^2$

Cesium Isotope	A_s 10^{-20} erg	$\|\psi(o)\|^2$ 10^{25} cm^{-3}
127	5896.401	2.608
129	6114.369	2.632
133	1522.568	2.638
134	1541.309	2.627
134m	287.185	2.670
137	1675.427	2.633
		Average 2.634

The resulting calculated values for β^2 are

$$\begin{aligned}
\beta^2(^{127}\mathrm{Cs}) &= 11.27 \times 10^{-2} + \beta^2(^{137}\mathrm{Cs}) \\
\beta^2(^{129}\mathrm{Cs}) &= 8.55 \times 10^{-2} + \beta^2(^{137}\mathrm{Cs}) \\
\beta^2(^{131}\mathrm{Cs}) &= 6.63 \times 10^{-2} + \beta^2(^{137}\mathrm{Cs}) \\
\beta^2(^{132}\mathrm{Cs}) &= 5.24 \times 10^{-2} + \beta^2(^{137}\mathrm{Cs}) \\
\beta^2(^{133}\mathrm{Cs}) &= 4.21 \times 10^{-2} + \beta^2(^{137}\mathrm{Cs}) \\
\beta^2(^{134}\mathrm{Cs}) &= 2.81 \times 10^{-2} + \beta^2(^{137}\mathrm{Cs}) \\
\beta^2(^{135}\mathrm{Cs}) &= 1.85 \times 10^{-2} + \beta^2(^{137}\mathrm{Cs}) \quad .
\end{aligned} \tag{89}$$

Here the value of ^{137}Cs is chosen as the reference point, since ^{137}Cs has a magic closed neutron shell with N = 82.

The nuclear deformation parameters can also be calculated from the intrinsic quadrupole moments according to the formula

$$Q_o = \frac{3}{(5\pi)^{\frac{1}{2}}} ZR_o^2 (\beta + 0.36 \beta^2) \quad . \tag{90}$$

Taking $\beta^2(^{137}\mathrm{Cs}) = 0.01 \times 10^{-2}$ as calculated from Eq. (90), numerical values can be obtained for the quantities in Eq. (89). These values are presented in Table IX and plotted against the mass number A in Fig. 19, together with the values obtained on the basis of Eq. (90).

Table IX. Values of β^2

Cesium Isotope	β^2 in 10^{-2}	
	From Isotope Shift	From Quadrupole Moment
127	11.28	---
129	8.56	---
131	6.64	1.07
132	5.25	1.08
133	4.22	0.00
134	2.82	0.20
135	1.86	0.01
137	0.01	0.01

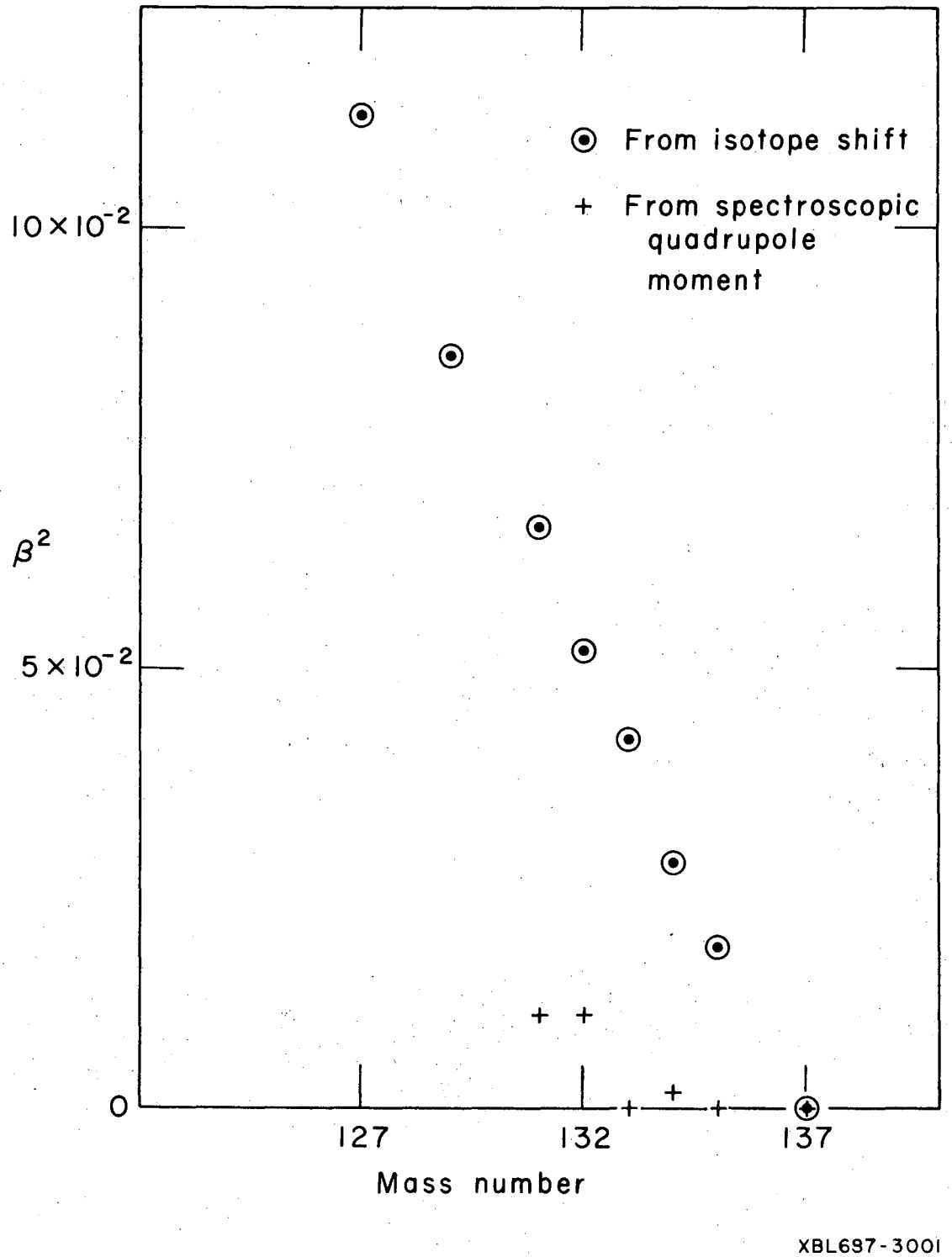

Fig. 19. Square of nuclear deformation parameter versus mass number.

VI. DISCUSSION

Both the presence of the finite though small isomeric shift between ^{134}Cs and ^{134m}Cs and the nearly complete cancellation of the mass effects seem to indicate that the observed isotope shifts arise essentially from the nuclear field effects. As is evident from Fig. 19, the nuclear deformation derived from the isotope shifts shows a steady increase with the increase of the number of neutron holes. This observation is in agreement with the theoretical prediction of the existence of a region of nuclear deformation among neutron deficient isotopes in the region $50 \leq Z \leq 82$ and $50 \leq N \leq 82$.[32,33] The experimental observation of deformed nuclei among the neutron deficient even isotopes of Xe,[34] Ba and Ce[35] also has a bearing on this point. Moreover, these deformed nuclei have ground-state bands characterized between rotational and vibrational, i.e. they are not permanently deformed. Since $\langle \beta_{vib} \rangle = 0$, the resulting intrinsic quadrupole moment will be, as can be seen from Eq. (90), much smaller than it would be if the nucleus were permanently deformed.

The above evidence seems to be a convincing argument in favor of the interpreation that the smallness of the observed shifts in the cesium isotopes is a result of the counteraction of the two field effects.

Acknowledgments

I thank the many people involved in bringing this work to a successful completion, especially:

Professor Richard Marrus for his support, guidance and encouragement.

Dr. Joseph Yellin for his constant help.

Eldred Calhoon of the Health Chemistry monitors for his valuable aid in handling the radioactive samples.

Mrs. Julia Taylor and Miss Nadine Kamada for typing the manuscript.

My fiancee, De-Jane.

This work was done under the auspices of the U. S. Atomic Energy Commission.

References

[1] H. Kopfermann, Nuclear Moments, (Academic Press, New York, 1958).

[2] G. Racah, Nature, Lond. 129, 723 (1932).

[3] J. E. Rosenthal and G. Breit, Phys. Rev. 41, 459 (1932).

[4] P. Brix and H. Kopfermann, Z. Physik 126, 344 (1949).

[5] E. K. Broch, Arch. Math. Naturv. 48, 25 (1945).

[6] A. R. Bodmer, Proc. Phys. Soc. A 66, 1041 (1953); Nucl. Phys. 9, 371 (1959).

[7] E. Fermi and E. Segre, Z. Physik 82, 729 (1933).

[8] P. Brix and H. Kopfermann, Nachr. Akad. Wiss. i. Goettingen, Math.-Phys. 2, 31 (1947).

[9] K. W. Ford, Phys. Rev. 90, 29 (1953).

[10] L. Wilets, D. L. Hill, and K. W. Ford, Phys. Rev. 91, 1488 (1953).

[11] A. R. Bodmer, Proc. Phys. Soc. A 67, 622 (1954).

[12] L. R. B. Elton, Nuclear Sizes (Oxford University Press, London, 1961).

[13] N . F. Ramsey, Molecular Beams (Oxford University Press, London, 1956).

[14] R. E. Trees, Phys. Rev. 92, 308 (1953).

[15] E. Fermi, Z. Physik 60, 320 (1930).

[16] R. Marrus and D. McColm, Phys. Rev. Letters 15, 813 (1965).

[17] R. Marrus, D. McColm, and J. Yellin, Phys. Rev. 147, 55 (1966).

[18] J. R. Zacharias, Phys. Rev. 61, 270 (1942).

[19] R. Marrus, E. Wang, and J. Yellin, Phys. Rev. Letters 19, 1 (1967).

[20] H. Kleiman, J. Opt. Soc. Am. 52, 441 (1962).

[21] G. H. Fuller and V. W. Cohen, Nuclear Moments, Appendix 1 to Nuclear Data Sheets, 1964.

[22] W. A. Nierenberg, H. A. Shugart, H. B. Silsbee, and R. J. Sunderland, Phys. Rev. 112, 186 (1958).

[23] J. Bauche (Lab. Aime Cotton, Orsay, France), private communication, April 1968.

[24] E. E. Fradkin, Soviet Physics - JETP 15, 550 (1962).

[25] H. Huehnermann and H. Wagner, Phys. Letters 21, 303 (1966).

[26] E. W. Otten and S. Ullrich, Z. Physik (1968) (to be published).

[27] H. Huehnermann and H. Wagner, Z. Physik 199, 239 (1967).

[28] F. Ackermann, E. W. Otten, G. zu Putlitz, A. Schenck and S. Ullrich, Phys. Letters 26B, 367 (1968).

[29] K. H. Althoff, Z. Physik 141, 33 (1955).

[30] G. Heinzelmann, U. Knohl, and G. zu Putlitz, Z. Physik 211, 20 (1968).

[31] H. Bucka, H. Kopfermann and E. W. Otten, Ann. Physik 4, 39 (1959).

[32] E. Marshalek, L. W. Person, and R. K. Shelline, Rev. Mod. Phys. 35, 108 (1963).

[33] K. Kumar and M. Baranger, Phys. Rev. Letters 12, 73 (1964).

[34] H. Morinaga and N. L. Lark, Nucl. Phys. 67, 315 (1965).

[35] K. Miyano, M. Ishihara, Y. Shida, H. Morinaga, T. Kuroyanagi, and T. Tamura, Nucl. Phys. 61, 25 (1965).